U.S. Department
of Transportation
**National Highway
Traffic Safety
Administration**

NHTSA

DOT HS 812 632

September 2018

Radar Congestion Study

DISCLAIMER

Suggested APA Format Citation:

Buller, W., Wilson, B., Garbarino, J., Kelly, J., Subotic, N., Thelen, B., & Belzowski, B. (2018, September). *Radar congestion study* (Report No. DOT HS 812 632). Washington, DC: National Highway Traffic Safety Administration.

1. Report No.	2. Government Accession No.	3. Recipient's Catalog No.
DOT HS 812 632		

4. Title and Subtitle	5. Report Date
Radar Congestion Study	September 2018
	6. Performing Organization Code: HOTO-1

7. Authors	8. Performing Organization Report No.
William Buller, Brian Wilson, Joseph Garbarino, Jack Kelly, Nikola Subotic, Brian Thelen, all Michigan Technological University, and Bruce Belzowski (UMTRI)	

9. Performing Organization Name and Address	10. Work Unit No. (TRAIS)
University of Michigan Transportation Research Institute 2901 Baxter Road Ann Arbor, MI 48109	11. Contract or Grant No. DTNH22-14-D-00329L-0006

12. Sponsoring Agency Name and Address	13. Type of Report and Period Covered
National Highway Traffic Safety Administration 1200 New Jersey Avenue SE. Washington, DC 20590	Final Report
	14. Sponsoring Agency Code

15. Supplementary Notes

16. Abstract

This study builds on prior work to characterize the environment in which automotive radars must operate, especially as systems with greater autonomy enter the market. Systems that operate well in environments without other radars may suffer significant degradation of performance in radar-congested environments. The results of this research provide an understanding of the levels of interference expected under different scenarios. This allows us to identify situations that require mitigation of radio frequency interference (RFI). Many techniques have been developed to mitigate RFI and several are discussed in this report. Some mitigation strategies rely on standards practiced by all the transmitters in the environment. This study identifies scenarios that require RFI mitigation and those strategies that require harmonization.

17. Key Words	18. Distribution Statement
automotive sensors, radar, mutual interference, active safety, autonomous vehicles, RFI, radio frequency interference	This document is available to the public through the National Technical Information Service, www.ntis.gov.

19. Security Classif. (of this report)	20. Security Classif. (of this page)	21. No. of Pages	22. Price
Unclassified	Unclassified	87	

Contents

List of Tables

List of Figures

List of Abbreviations and Acronyms

ADAS	Advanced Driver Assist System
AEB	automated emergency braking
BPSK	binary phase shift keying
CF	channel fraction
CFAR	constant false alarm rate
clutter	objects illuminated by radar, which the system needs to ignore
CW	continuous wave
dB	decibels
dBm^2	decibel meters squared (log unit of area)
DBF	digital beam-forming
DF	duty factor
ego vehicle	vehicle under test
f_N	noise factor
FCW	forward collision warning
FOR	field of regard
FOV	field of view
Hz	Hertz (cycles per second)
interferer	vehicle operating a radar which may interfere with ego vehicle's radar
LFM	linear frequency modulated waveform
MOSARIM	MOre Safety for All through Radar Interference Mitigation
PD	probability of detection
PFA	probability of false alarm
POI	probability of intercept
PSK	phase shift keying
radar	radio frequency detection and ranging
RCS	radar cross section
RF	radio frequency
ROC	receiver operating characteristic
RX	receiver
SINR	signal to interference plus noise ratio
SNR	signal to noise ratio
SOC	system on chip
SWAP+C	size, weight, and power plus cost
target	object of interest illuminated by radar
TX	transmitter

1 Executive Summary

The automotive industry is undergoing a fundamental transformation, made possible by a multitude of advancements in electronic, communication, and remote sensing technologies. Automobiles are being developed with varied levels of autonomy to increase efficiency, reduce congestion, improve safety, and provide reliable transportation to communities that formerly would be dependent on others for assistance. Consider, for example, the following press release from 2016:

> *The U.S. Department of Transportation's National Highway Traffic Safety Administration and the Insurance Institute for Highway Safety announced today a historic commitment by 20 automakers representing more than 99 percent of the U.S. auto market to make automatic emergency braking (AEB) a standard feature on virtually all new cars no later than NHTSA's 2022 reporting year, which begins Sept 1, 2022. "U.S. DOT and IIHS announce historic commitment of 20 automakers to make automatic emergency braking standard on new vehicles."* (NHTSA & IIHS, 2016)

Vehicles that are designed to sense their surroundings and navigate traffic safely, may reduce the risks posed by human errors in their operation. Such vehicles rely on a host of active and passive sensing systems; an important class of sensors for this application is radio frequency detection and ranging systems (RADAR). The technology is old enough that the word radar is used in daily language.

Radar is particularly well suited for detection and tracking of objects for collision avoidance systems. Radar is an active sensing technology, which can function day or night, and in all weather. The parameters of a radar can be tuned to the detection and tracking problems of navigation guidance and collision avoidance. Recent developments in a multitude of technologies have facilitated the availability of radar systems highly capable for automotive navigation, with relatively low size, weight, and power plus cost (SWAP+C). As with any active sensor, a radar transmits energy to understand its local environment. The operation of multiple active systems can result in an environment where each sensor is subject to energy emitted by other transmitters, as well as its own. This situation results in mutual interference for the sensing systems, and degrades their performance.

This radar congestion study characterizes the environment in which automotive radars must operate, as market penetration of radar-equipped vehicles grows. Systems that operate well in environments with few other radars may suffer significant degradation of performance in radar congested environments. The results of the study show levels of interference based on operation of current systems in congested environments will be significant. In scenarios with many vehicles operating radars in the 76-81 GHz band, the power from other radars will likely exceed the power of echoes from targets needed for specified performance by several orders of magnitude.

The modeling and simulation work focused on two questions:

- How much power does a given radar receive from other radar transmitters?
- How does this impact the performance of a collision warning system?

The first question was addressed by developing a model for nominal automotive radars and computing the amount of power overlapping in space, time, and spectrum. This work is done theoretically, assuming free space propagation of radio frequency (RF) waves.

The second question was addressed by introducing the power computed for the interference, as noise, into a system simulation. This approach is common in past studies, and assumes the waveforms of the interfering radar are substantially different, so that their mutual energy does not correlate. This approach is taken, in part, because it requires a minimum of assumptions about the signal processing chain behind the receiving radar's front end. Further, there are a great deal of possible combinations, and interactions, that require empirical evaluation.

To quantify possible system impacts, the processing functions were based on a generic model developed in cooperation with industry professionals and simulated in MATLAB's Automated Driving System Toolbox. For this reason, the current study does not capture the system impacts which depend on the multitude of interactions possible with different waveforms, which could be addressed through further analysis and empirical tests. Nevertheless, with these caveats, the simulations in this study suggest radar performance could be significantly impacted.

The results of this research provide an initial understanding of the levels of interference expected under different scenarios. Scenarios are selected to represent typical traffic situations in which mitigation of radio frequency interference (RFI) would improve radar performance. The report provides an understanding of the level of interference that systems face, and what strategies may provide sufficient mitigation.

Many techniques have been developed for the purposes of mitigating RFI, and are discussed in this report. The report focuses on those strategies reported as practiced by the industry, as well as others, which show significant promise. Some mitigation strategies rely on common operating standards practiced by all the systems in the environment (harmonization). This study identifies scenarios requiring significant RFI mitigation. The study tabulates the effectiveness of mitigation strategies, and identifies those which involve harmonization across transmitters.

Based on the analysis here, using reasonable specifications for automotive radars, it is shown that automotive radars, operating in congested environments, will face significant interference. For example:

- In the case of opposing traffic on a two-lane highway, assuming that the radars use randomly selected carrier frequencies, an automotive radar will encounter power from other radars far greater than the echoes of its own transmissions needed to track other vehicles. The interference approaches four orders of magnitude, or nearly 40 dB, greater than echoes typical of a reference target, as specified for the system.
    - Under simulation, the range at which the radar develops a track that persists through to collision, was reduced to a fraction, 11 percent, of what is observed without interference.
- In the case of radars which face rearward (such as blind-spot detection systems), these units are vulnerable to the direct arrival of forward collision avoidance radars that utilize higher power and antenna gain. Our analysis shows these units could experience interfering power from a forward collision avoidance radar that is nearly five orders of magnitude, or 50 dB, greater than the reflections from their specified reference target.

Therefore, it is important that automotive radar makers consider techniques capable of mitigating interference to levels that allow the system to perform as specified. The automotive safety testing community should consider this side effect of active sensors in its assessment of automotive systems employing active sensors.

The study here evaluated the practices and trends in the industry through a survey of literature, and interviews with manufacturers. Mitigation strategies, with estimates of performance, are tabulated. The principal mitigation techniques practiced in industry are listed below, along with estimates of effectiveness:

- A technique focused on detecting interference and repairing receiver results in time domain can reduce interference by 3 to 20 dB, depending on the specifics of the interfering systems.
- Stretch processing, which lowers the systems' overall signal to noise ratio, can reduce levels of interference by 10 dB.
- Digital Beam Forming, is becoming more common with system-on-chip (SOC) architectures, allows the radar to restrict the receiver's spatial field of view. Based on current designs, this should allow many systems to put the majority of the interfering systems at the antenna array's side lobe levels, and reduce the interference by 5 to 10 dB.
- Specific polarization following the radar location on the automobile: front, rear, or side. The idea is that front-facing radars, for example, could be selected so as to reduce interference levels when confronting each other in opposing traffic. This approach can mitigate interference levels by 10 to 15 db; however, it involves harmonization across the industry to a common convention.
- The formidable interference levels that a rear-facing radar will experience from illumination by more powerful forward collision radars suggests that polarization conventions alone will not be sufficient. With all radars operating at W-band, one solution would be to divide the 76-81 GHz spectrum, for operation of forward-facing and rear-facing radars. This approach can mitigate up to 60-80 dB, but also involves harmonization across the industry.

Results from this study are reported based on stochastic models of interference power and the impact on a generic system in simulation. The estimates of the interference power are tabulated, and compared to the power associated with ambient clutter (reflections from the road), and a reference target. If the interference power is near the level of power reflected from targets of interest (other cars, pedestrians, bicyclists, etc.), then the radar systems is operating in an environment that will degrade its performance, if mitigation strategies are not employed.

2 Introduction

2.1 Assisted driving and active safety radars

Increased occurrence of radar interference has negative impacts on the performance of automotive radars and the assisted driving systems that rely on them. Assisted driving systems are becoming embedded in more vehicles as the technology base matures. These systems promise greater safety, reduced congestion and greater situation awareness for drivers. In many cases, these systems use active and passive sensors along with wireless communications (Sturm, Sit, Braun, & Zwick, 2013), as shown in Figure 1. Up to this point, attention has been paid to

making the technology operate and not much consideration has been paid to the mutual impact of the highway infrastructure and safety systems when deployed in large numbers. The effect of operating large numbers of radars in the same spectrum and in close proximity raises the possibility that their operation may cause mutual interference.

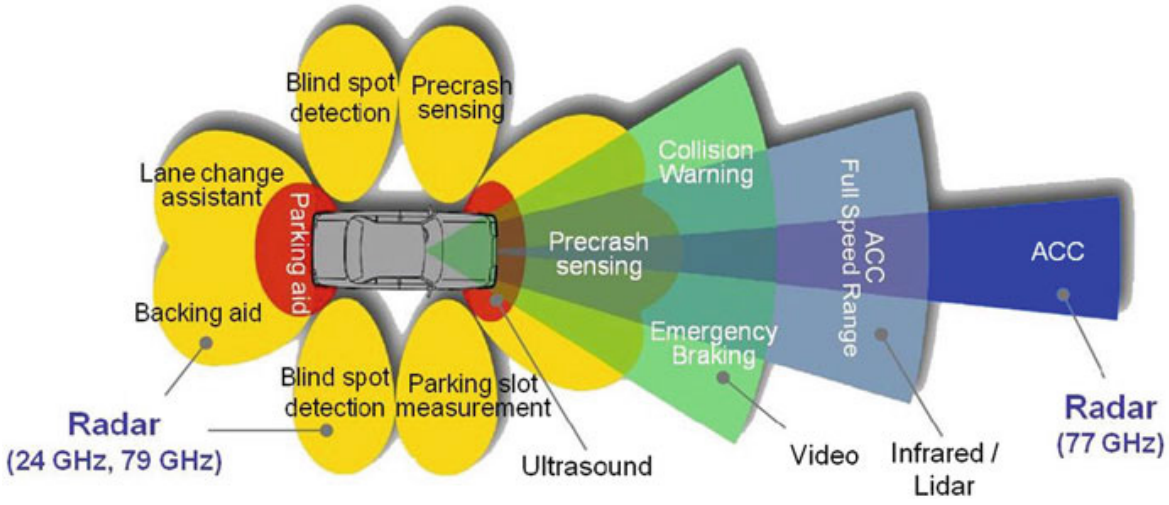

Figure 1:- An example deployment of multiple radar sensors used for active safety and assisted driving systems (Kissinger, 2012)

2.2 Recent changes to spectrum allocation

An important change in the allocation of the automotive radar spectrum has occurred following the start of this study. The United States Federal Communications Commission has expanded the spectrum available for vehicular radars, to include the entire 76-81 GHz band and to transition radars out of the 24 GHz band. This change makes for a consistent allocation of spectrum available internationally, avoiding the need to customize the radars in vehicles for different markets. The analysis performed in this study is, thus, focused on systems operating in the 76-77 and 76-81 GHz.

The text from the FCC announcement appears below (Grace, 2017).

> *Media Contact:*
> *Neil Grace, (202) 418-0506, neil.grace@fcc.gov*
> *For Immediate Release*
>
> *FCC UNLOCKS NEW AIRWAVES FOR VEHICULAR RADAR USE*
> *Spectrum Will Enhance Crash Avoidance and other High-Tech Safety Features*
>
> *WASHINGTON, July 13, 2017 – The Federal Communications Commission today expanded the spectrum available for vehicular radars that are used for a variety of purposes, including safety applications like collision avoidance and adaptive cruise control. Access to this additional spectrum will enable continued innovation in this space, allowing these radars to better distinguish between objects in areas close to the vehicle. This action will improve performance for applications such as lane change warnings, blind spot detection, parking aids, "stop and follow," "stop and go," autonomous braking, and pedestrian detection.*

The Commission's action expands the current 76-77 GHz spectrum allocation to include the entire 76-81 GHz band and transitions radars out of the 24 GHz band. This is consistent with the spectrum that is available internationally, avoiding the need to customize the radars in vehicles for different markets.

The Order also permits the use of this band for fixed and mobile radars at airports that are used for important safety applications, such as the detection of debris on runways that could harm aircraft on take-off and landing. Making the entire 76-81 GHz band available at airports will allow for improvements to these existing technologies as well as promote the development of new safety applications, such as wingtip radars that can help aircraft avoid collisions with objects while moving on airport grounds.

Action by the Commission July 13, 2017 by Report and Order (FCC 17-94). Chairman Pai, Commissioners Clyburn and O'Rielly approving and issuing separate statements. ET Docket No. 15-26

2.3 Radars and mutual interference

Radar is inherently a wave sensing measurement and subject to constructive and destructive combinations of radar transmissions. Therefore, interference is expected in environments dense with reflective targets, as well as environments with similar transmitters. This section discusses the growing role of radar in automotive applications and how that growth increases the occurrence of radar interference.

Radars use knowledge of radiated signals to identify echoes and estimate the range and speed of objects in the environment. These echoes are not perfect copies of the original signal, but a sum of multiple returns that constructively and destructively interfere with the signal. It is important to understand that returns from objects illuminated by radar fluctuate, especially when the relative range, aspect and other objects in the scene change. With multiple radars operating in near proximity and an environment of multiple sources of scattering, the performance of each radar degrades as the interference level rises.

The research conducted here shows the levels of mutual interference expected when operating many vehicles with automotive radar in dense traffic produces a challenging environment for successful radar operation. A generic automotive radar specification was generated, based on a survey of literature and manufacturers specifications, and then assessed as reasonable, by engineers from Delphi and Bosch. Automotive radars are typically evaluated for detection performance on a reference target. In this study, the reference target for the automotive radar has a cross-section of $10\ dBm^2$, and is observed at a range of $175\ m$. In scenarios with opposing traffic, and cars spaced at an average of $15\ m$, the power expected on a radar's receiving antenna is computed to be approximately 30 decibels (dB) above the power expected from the return of the reference target. Typical radar operation requires false alarm rates to be kept near or below 1 per 1 million samples. At this false alarm rate, to achieve a 90 percent probability of detection, a radar needs approximately 10 dB of signal to noise ratio (Tyson, 2013). In the case of radar interference limiting system performance, 10 dB of signal to interference is necessary to operate the system without suffering an intolerable error rate. Thus, to achieve the specified performance, the system must be able to mitigate approximately 40 decibels of interference.

2.4 Interference mitigation strategies

There are several key issues that need to be addressed when proposing RFI mitigation techniques beyond suppressing interference. Automotive radars are relatively low power transmitters intended to detect other vehicles for collision avoidance. The precision of the range estimate, ρ, for a radar is based on the bandwidth, B, of its waveform. Greater bandwidth provides better range resolution. The resolution statement for a radar is expressed as in the equation below, where the constant c is used for the propagation speed of light.

$$\rho = \frac{c}{2B} \qquad \text{Equation 1}$$

The speed of light is approximately $3 \times 10^8\ m/s$. So if a radar designer wants the system to resolve targets as small as 1 meter, then the bandwidth of the waveform should be $1.5 \times 10^8\ cycles/s$, or 150 MHz. To obtain good resolution of the unambiguous Doppler shift (thus, the radial speed of the target), the radar benefits from a waveform where the shift in frequency can be observed over many samples (high duty cycle). This leads many automotive radar designs to the use of a linear frequency modulated waveform.

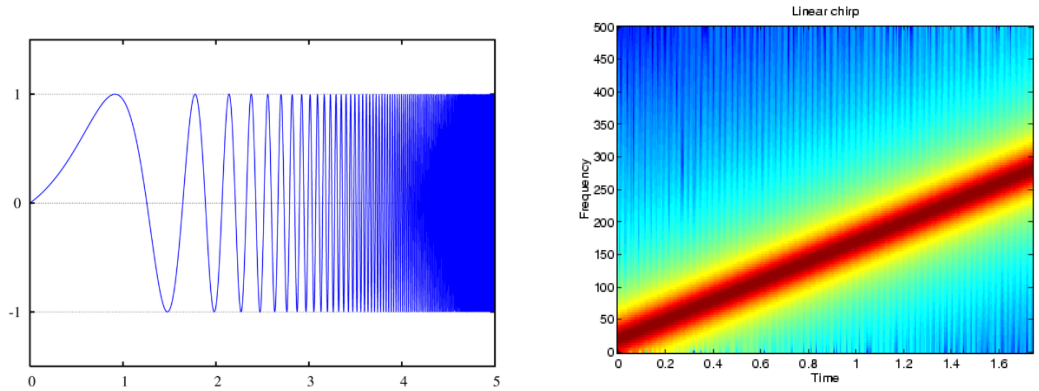

Figure 2: A linear frequency modulated waveform, or chirp, is shown on the left, as a time domain signal. The spectrogram at right shows the spectral power in frequency, increasing linearly over time.

Many automotive radars employ linear frequency modulated waveforms for a variety of reasons.

- High time-bandwidth product: because the waveform changes frequency, it covers a large bandwidth, over a long time, providing both range and Doppler resolution
- Strong Doppler tolerance: the waveform is robust to under sampling at the analog to digital conversion stage, because minor shifts in timing will result in a detection with only a minor shift in frequency
- Smooth phase modulation – unlike digital phase shift keyed waveforms, the continuous phase transition of the LFM does not introduce unnecessary noise into the receiver

Other automotive radars use frequency shift keying, where the frequency is varied, according to a pre-determined code. This type of waveform also allows the radar to achieve a high time-bandwidth product, but typically increases the noise factor, because of electronic switching, for the radar.

Many automotive radars operate in the 76 to 77 GHz and often use upwards of 200 MHz bandwidth. If each radar needs 200 MHz bandwidth of a total of 1000 MHz available, then only 5 radars can operate in a given area and that is without any guard bands. The ranking list identified from MOre Safety for All through Radar Interference Mitigation (MOSARIM) is shown in Table 1. This list was used as a starting point for the current study, and the updated evaluation appears in Table 2.

Table 1: Ranking list of mitigation techniques. The reference numbers refer to the mitigation techniques' appearance in the MOSARIM study tables. Items in green were evaluated as being most valuable for interference mitigation. Items in yellow are evaluated as being of secondary value. Source: from Kunert, 2012

Ref.	Title
T3.1	CFAR (constant false alarm rate) for interference mitigation
T6.5	Detect interference and change transmit frequency range of chirps
T2.1	Using pauses of random length between chirps or pulses
T3.4	Application of driving direction specific pre-defined frequency band separation
T6.2	Detect interference and repair Rx results (Time domain)
T2.2	Using random sequence of chirp types (Up-chirp, Down-chirp, CW-Chirp)
T5.4	Digital beam forming
T6.4	Detect interference and change timing of transmit chirp or pulses
T1.2	Specific polarization following the radar location (frontal rear side)

The mitigation strategies listed in Kunert (2012) come with trade-offs. For example, the first mitigation strategy suggests the use of a constant false alarm rate (CFAR) detector. This was given a positive evaluation in MOSARIM, but it should be noted, this is promising for mitigating false alarms, but has significant side effects. The CFAR will ensure that the false alarm rate does not erupt in the presence of high noise or interference; however, this is achieved by reducing the probability of detection.

Some of the techniques consider randomizing of time multiplexing which may not provide mitigation in high clutter environments – if there are reflections at many delay times, the interfering signal will show up regardless of the transmitting schedule. Other strategies such as the second in the list, which is referred to as "sniff-and-avoid" in cognitive radio applications, may be successful in low-congestion operation, but in highly congested environments this may greatly degrade radar performance.

This study included a survey with automotive radar industry representatives to gain a better understanding of the industry view of the threat posed by mutual interference for their radar systems, and the steps being taken to mitigate the threat. Based on the results of that survey and examination of the literature, the table first prepared in the MOSARIM study can be updated to focus on the techniques that are reported by the industry, and result from developments in technology, and the market.

The updated table of countermeasures appears as Table 2, where row headings in blue identify techniques that involve adherence to convention across the industry (harmonization). Each of the rows in this table is given further comment as follows:

- T6.2: Detecting interference and repairing receiver results may be implemented in a multitude of ways. The techniques with the most promise are in the time domain waveform. One implementation uses prior knowledge of transmissions by other radars. In this implementation, a detector, matched for other radars, identifies pulses that contain high levels of interference and flags them, so that they are elided and do not pollute processing downstream. Performance of countermeasures in this class are subject to the density of other systems, the fidelity and completeness of the systems database of other radar transmissions, and may still be vulnerable to RFI from a unit with similar parameters.
- The radar congestion study finds that many automotive radar makers employ a technique called stretch processing (Levanon & Mozeson, 2004). This is often done so that the receiver can use a lower rate analog to digital converter, which is a significant cost saving. The beneficial side effect is that the receiver uses less bandwidth, and reduces spectral overlap, perhaps by as much as a factor of 10.
- T5.4: Although not tested during the MOSARIM study, digital beam forming is becoming a prominent feature in newer automotive radar systems for the benefit of finer angular resolution. The narrowed angular response of the antenna array benefits the receiver by spatially limiting interference. The amount of interference reduction is constrained by the number of elements in the receiving antenna array, and the directionality of interference sources. Newer antenna arrays are being designed with a greater number of elements, and this is reflected in the increased estimate of interference reduction, over that reported in MOSARIM.
- T1.2: The idea of specifying polarization to mitigate interference is reported by MOSARIM. This can be done with linearly and circularly polarized transmitters. For linear systems, the transmitting antenna must all be rotated about their axis (a.k.a. clocked) in a way as to present energy to other systems in an orthogonal polarization state. Circular polarized radars, using the same handedness, are also orthogonal for this application if they all use the same handedness. This is because a radar, for example, using a left-handed circularly polarized transmit antenna, CPLH, detects reflections with a right-handed circularly polarized receive antenna, CPRH. The CPLH waveforms will be greatly attenuated at the receive antenna. The reduction for the response of a linear antenna to the transmission of a circularly polarized radar, and vice versa, is 3 dB.
- The radar congestion study finds that a rear-facing radar will experience illumination by more powerful forward collision radars which may overwhelm the radar's ability to operate at even a degraded level. With all radars operating at W-band, one solution would be to divide the 76-81 GHz spectrum, for operation of forward and rear-facing radars. If this approach is implemented with harmonization across the industry, it can mitigate interference between forward and rearward radars by 60-80 dB.

Table 2 –Radar Congestion Study rankings for RFI mitigation countermeasures reported by industry, including those evaluated MOSARIM study. Items in green are practiced by multiple makers in the industry. The items in blue involve harmonization.

ID	Counter Measures	Interference Reduction	Comment
MOSARIM T6.2	Detect interference and repair Rx results (time domain)	3-20 dB , depending on environment	The influence of fast or slow crossing FM chirps still needs further investigation on mitigation margin impact
RCS Study	Stretch processing	10 dB	The main cost of the stretch processing technique is the loss of signal to noise ratio. So long as the interference is at least 10 dB greater than the noise, the technique is advisable.
MOSARIM T5.4	Digital Beam Forming	5-10 dB	Mitigation effect depends on beamwidth (space domain), based on number of elements in receiver array
MOSARIM T1.2	Specific polarization following the Radar location (frontal, rear, side)	10-15 dB for co pol - systems using the same convention	This is already partially used for ACC radars that have 45 degree slant linear polarization (reduced interference from oncoming radars by 15 dB). Involves harmonization.
RCS Study	Spectrum division following the Radar location (frontal, rear, side)	60 to 80 dB for forward and rear-facing radars in traffic	As all automotive radars move to W-band, 76-81 GHz, splitting the spectrum could reduce interference between forward and rearward looking radars by 60 to 80 dB. Involves harmonization.

Notably removed from the original table, which appears in Appendix: Evaluation of Mitigation Strategies From MOSARIM, is the technique labelled as T3.1: The application of a CFAR. This was considered as a technique for interference mitigation at the time of the MOSARIM study; however, it should not be considered as such for autonomous vehicle operation in scenarios with persistent RFI. It is a valid technique for mitigating false alarms, but inherently adds risk for desensitizing the system.

3 Literature Review and Prior Studies

Automotive radars operating in traffic face an environment rich with interference from the direct arrival of other radar transmissions as well as their reflections from objects in the environment. Radio frequency interference is, thus, impacted by the density of vehicles using radar in the same band, as well as the density of objects in the environment. The study of existing literature and prior work reveals that the community of interest, which includes industry and academia, has increased its interest in mitigating interference for automotive radar systems as the number of systems grows.

The literature search focused on four areas.

- General physics of the congestion problem
- Modeling and simulation of congested environments
- Testing and performance measures for radar in a congested environment
- Mitigation techniques

Important works in each of these four areas are highlighted in the following sections. This review is not intended to be exhaustive, but provides a snapshot of the current body of knowledge. Each section leads with a summary of what is relevant to the current study.

3.1 General physics of the congestion problem

While radar interference is a well understood phenomenon and studied for many decades, the concern of when and how this will impact the development of advanced driver assist systems and autonomous vehicles is relatively new. The references highlighted in this section address this point, and provide resources that are used to help develop our models of the radars and the operating environment used in this study.

Heuel, S. (2016). Automotive radar sensors must address interference issues. *Microwave Journal, 59*(12), pp. 22-36.

> ***This reference is used in modeling parameters of automotive radars and experimental design.***
>
> *There are mainly two different types of waveforms used in today's automotive radar sensors. Blind Spot Detection (BSD) radars often use the Multi-Frequency Shift Keying (MFSK) radar signal and operate mainly in the 24 GHz band. Radars operating in the 77 GHz or 79 GHz band often make use of Linear Frequency Modulated Continuous Wave (LFMCW) signals or Chirp Sequence (CS) signals, which are a special form of LFMCW signals.*
>
> *Considering that 72 million new cars are registered each year with a potential average of three (or more) automotive radar sensors per car, about 200 million more automotive radar sensors could be on the streets in the not too distant future. Consequently, the 24 GHz and 76 to 81 GHz spectrum will be heavily occupied. Automotive radar sensors will need to cope with mutual interference and offer signal diversity and interference mitigation techniques.*

Jain, V., & Heydari, P. (2013). *Automotive radar sensors in silicon technologies*. New York: Springer New York**,** 1-100.

> ***This reference is used in modeling the parameters of automotive radars in this study.***
>
> *This book presents architectures and design techniques for mm-wave automotive radar transceivers. Several fully-integrated transceivers and receivers operating at 22-29 GHz and 77-81 GHz are demonstrated in both CMOS and SiGe BiCMOS technologies. Excellent performance is achieved indicating the suitability of silicon technologies for automotive radar sensors. This book bridges an existing gap between information available on dependable system/architecture design and circuit design. It provides the background of the field and detailed description of recent research and development of silicon-based radar sensors. System-level requirements and circuit topologies for radar transceivers are described in detail. Holistic approaches towards designing radar sensors are validated with several examples of highly-integrated radar ICs in silicon technologies. Circuit techniques to design millimeter-wave circuits in silicon technologies are discussed in depth.*

Brooker, G. M. (2007). Mutual interference of millimeter-wave radar systems. *IEEE Transactions on Electromagnetic Compatibility, 49*: 170-181.

This reference is used to understand the types of errors that may arise in systems with unmitigated interference, and informs the studies recommendations.

This paper examines the probability that any millimeter-wave radar systems will interfere mutually by considering spatial, temporal, and operational frequency-related overlaps. It examines the nature and magnitude of the interference under different conditions and for different sensor types before concluding that in an overlapping frequency band, the probability that interference will occur is high. It goes on to demonstrate that, though there are some forms of interference that can be identified and controlled, there are others which are impossible to isolate, (i.e., the interference overlapping in space, time, and frequency) resulting in degraded target detection performance and tracking.

Maksimov, M. V., Bobnev, M. P., Shustov, L. N., Krivitskii, B. K., Gorgonov, G. I. Ilin, V. A., & Stepanov, B. M. (1979). *Radar anti-jamming techniques*. Norwood, MA: Artech House. 1-420.

Natural, intentional, and inadvertent mutual interference is described. Attention is given to methods of protecting systems from jamming. Emphasis is placed on techniques of protecting receivers from overloads, cancellation of radio interference, spatial, polarization, frequency, phase, time, amplitude, structural, amplitude-frequency, and space-time selection of signals in a noise background, and the complete utilization of information for enhancing noise immunity.

Goppelt, M., Blöcher, H.-L., & Menzel, W. (2010). Automotive radar – investigation of mutual interference mechanisms. *Advances in Radio Science,* 8: 55-60.

In the past mutual interference between automotive radar sensors has not been regarded as a major problem. With an increasing number of such systems, however, this topic is receiving more and more attention. The investigation of mutual interference and countermeasures is therefore one topic of the joint project "Radar on Chip for Cars " (RoCC) funded by the German Federal Ministry of Education and Research (BMBF). RoCC's goal is to pave the way for the development of high-performance, low-cost 79 GHz radar sensors based on Silicon-Germanium (SiGe) Monolithic Microwave Integrated Circuits (MMICs). This paper will present some generic interference scenarios and report on the current status of the analysis of interference mechanisms.

John, A., & Schipper, T. (2012, December 21). MOre Safety for All by Radar Interference Mitigation D5.4 – Conclusion and outlook how to solve still open challenges (Part 4 of 4 parts. Report No. MOSARIM No. 248231). Brussels, Belgium: European Commission. Available at https://cordis.europa.eu/docs/projects/cnect/1/248231/080/deliverables/001-Deliverable54final.pdf

This reference is used as the initial set of mitigation strategies for evaluation in this study.

This report provides an overview of all the test campaigns conducted during the MOSARIM projects. All relevant information on test setup, measurements conducted and participants involved in the campaigns are given.

Due to IPR and NDA reasons not all sensor data is made available by the partners and interference impact is therefore mainly evaluated on a qualitative level. Even this evaluation in result matrix form with different classes (i.e., interference below 2dB / between 2 dB and 10 dB / above 10 dB over the victim receiver noise floor) is still confidential on consortium partner level and restricted for public dissemination. This deliverable is therefore submitted in two versions, the public, referred to in this study, and a confidential one.

Fischer, C., Blöcher, H. L., Dickmann, J., & Menzel, W. (2015). Robust detection and mitigation of mutual interference in automotive radar. In *Proceedings of the 2015 16th International Radar Symposium*, June 24-26, 2015, Dresden, Germany, pp. 143-148.

Active safety functions are being integrated into more and more cars. Many of these rely on radar sensors as a source of information about surrounding objects. Based on this information, for example, emergency braking maneuvers are initiated. This requires a very high reliability of the provided data. In the long term, these requirements will become even stricter as highly automated driving comes into play. In the near future, this will result in a high density of radar sensors operating simultaneously and in close proximity. This constellation generates mutual car-to-car interference if no precautions are taken. At present, efforts in measures to mitigate the interference concentrate on time-frequency signal processing. Spatial filtering using digital beamforming is another powerful method. This paper aims to cover the chain of interference, from the basic principles of waveform interaction in a radar sensor's receiver stage, up to mitigation techniques and consequences for signal processing in the presence of interference.

Sarabandi, K., Li, S. I., & Nashashibi, A. (1997, November). Modeling and measurements of scattering from road surfaces at millimeter-wave frequencies. *IEEE Transactions on Antennas and Propagation*, 45(11), pp. 1679-1688.

This reference is used in estimating the clutter level in this study.

Millimeter-wave radar-based sensors are being considered for a number of automotive applications including obstacle detection and collision warning, true-speed, and road-surface recognition. The interaction of electromagnetic waves with asphalt road surfaces, possibly covered with ice or water, at millimeter-wave frequencies is studied. First, an experimental procedure for determining the effective dielectric constant of bituminous mixtures used in road-surface constructions is developed. In this procedure, the effective dielectric constant is derived using a simple inverse-scattering algorithm to the measured radar cross sections of cylindrical specimen of a standard asphalt mixture. Then the vector radiative transfer equation is used to formulate the scattering from a multilayer medium representing an ice- or water-covered asphalt surface. The University of Michigan polarimetric 94-GHz radar

system was deployed for characterizing the polarimetric backscatter responses of asphalt surfaces under many physical conditions near grazing incidence angles (70°-88°). The measured backscatter coefficients and parameters of co-polarized phase difference statistics of a dry asphalt surface with smooth interface at one incidence angle were used to derive the phase and extinction matrices of the asphalt medium. The experimentally determined phase and extinction matrices are substituted in the radiative transfer formulation to predict the scattering from asphalt surfaces under all conditions. Excellent agreement between theoretical predictions and measured quantities is obtained

3.2 Modeling and simulation of congested environments

3.2.1 Estimating interference power

Simulation is important in the development of systems, so there is great interest in this area, and with increasing concern about interference, there are many models being developed. Many of the models in the literature develop statistical results by performing large numbers of trials with randomized initial conditions (Monte Carlo simulation), which is computationally expensive, and may fail to identify the importance of the contributing factors. These approaches are represented in the first three of the references highlighted in this section.

The remaining references in this section were used to develop the method to estimate the interference levels from a stochastic geometric model. The approach taken by the researchers for this study follows the stochastic geometric model, using Poisson point processes, which is particularly well suited for modeling distributions of vehicles in traffic (Haenngi & Ganti, 2008), and considers how to adjust the performance curve for a system in simulation.

Schipper, T., Prophet, S., Zwirello, L., Harter, M., Reichardt, L., & Zwick, T. (2013). Simulation framework for the estimation of future interference situations between automotive radars. In *2013 IEEE Antennas and Propagation Society International Symposium Proceedings*, July 7-13, Orlando, FL, pp. 2103-2104.

Interference between automotive radar systems is becoming an important topic of research today, since the density of automotive radars is rising continuously. However, the total amount of cars equipped with radar is still below one percent. This paper introduces a method to predict future interference conditions between automotive radars for higher penetration rates and presents selected results.

Goppelt, M., Blöcher, H.-L., & Menzel, W. (2011). *Analytical investigation of mutual interference between automotive FMCW radar sensors*. 2011 German Microwave Conference, March 14-16, 2011, Darmstadt, Germany, pp. 1-4.

Radar sensors are key components of modern driver assistance systems. Mutual interference was identified as a problem of increased importance because of the appearance of safety functions and the increasing rate of vehicles equipped with radar sensors. This paper describes mutual interference between automotive FMCW radar sensors. Analytical formulas were derived to be able to calculate the probability for ghost targets and the interference power per frequency bin. The results of the analytical calculations are compared with simulation results on the basis of a simple interference scenario with interference from an oncoming vehicle.

Schipper, T., Harter, M., Zwirello, L., Mahler, T., & Zwick, T. (2012). Systematic approach to investigate and counteract interference-effects in automotive radars. In *Proceedings of the 9th European Radar Conference*, October 28-November 2, 2012, Amsterdam, 190-193.

> *Considering the fast-growing market for automobile radars, a comprehensive investigation of interference between these radars is an essential step towards very high radar penetration rates with a maximum of system-to-system isolation. The MOSARIM project, funded by the European Commission, addresses this topic. The paper presented here introduces a multisystem radar simulator with focus on interference investigation and mitigation, including a scenario editing tool, a wave propagation simulator as well as the organization and post processing in Matlab. The simulation approach is demonstrated on the basis of a simple dynamic traffic scenario. Simulations and references underline the validity of the introduced approach.*

Haenggi, M., & Ganti, R. K. (2009). Interference in large wireless networks. *Foundations and Trends in Networking*, *3*(2), pp.127-248.

> *Since interference is the main performance-limiting factor in most wireless networks, it is crucial to characterize the interference statistics. The two main determinants of the interference are the network geometry (spatial distribution of concurrently transmitting nodes) and the path loss law (signal attenuation with distance). For certain classes of node distributions, most notably Poisson point processes, and attenuation laws, closed-form results are available, for both the interference itself as well as the signal-to-interference ratios, which determine the network performance.*

Daley, D. J., & D. Vere-Jones (2003). *An introduction to the theory of point processes: Volume I: Elementary theory and methods* (Second Edition). New York: Springer-Verlag. P. 491.

> ***This reference is used in estimating the traffic density and interference level in this study.***
>
> *Point processes and random measures find wide applicability in telecommunications, earthquakes, image analysis, spatial point patterns, and stereology, to name but a few areas. The authors have made a major reshaping of their work in their first edition of 1988 and now present their* Introduction to the Theory of Point Processes *in two volumes with sub-titles "*Elementary Theory and Models*" and "*General Theory and Structure*."*

Al-Hourani, A., Evans, R. J., Kandeepan, S., Moran, B., & Eltom, H. (2016). *Stochastic geometry methods for modeling automotive radar interference.* arXiv:1607.02434

> ***This reference is used in estimating the interference level in this study.***
>
> *As the use of automotive radar increases, performance limitations associated with radar-to-radar interference will become more significant. In this paper we employ tools from stochastic geometry to characterize the statistics of radar interference. Specifically, using two different models for vehicle spatial distributions, namely, a Poisson point process and a Bernoulli lattice process, we calculate for each case the interference statistics and obtain analytical expressions for the probability of successful range estimation. Our study shows*

that the regularity of the geometrical model appears to have limited effect on the interference statistics, and so it is possible to obtain tractable tight bounds for worst case performance. A technique is proposed for designing the duty cycle for random spectrum access which optimizes the total performance. This analytical framework is verified using Monte-Carlo simulations.

3.2.2 **Radar system trends**

"Prediction is very difficult, especially if it's about the future." - Niels Bohr

The literature has much to say on the topic, but perhaps the greatest lesson in this area is what is learned anecdotally talking to industry. The principal driver in this very competitive market remains the minimization of size, weight and power with cost (SWAP-C). The most important development from the perspective of this study is the prediction that the manufacturing of radars with greater signal processing capabilities will make digital beamforming available in platforms with reduced SWAP-C. The industry uses terms such as 3D radar, or holographic radar, to describe systems that can take advantage of an array of receiving elements and memory to allow coherent processing within the radar and provide higher resolution tracking of objects and reduced interference.

Wiesbeck, W., Sit, L., Younis, M., Rommel, T., Krieger, G., & Moreira, A. (2014). Radar 2020: The future of radar systems. In *Proceedings of the IEEE International Geoscience Remote Sensing Symposium*, Milan, July 26-31, 2015, pp. 188–191. DOI: 10.13140/RG.2.1.3811.2480

The first radar has been patented 110 years ago. Meanwhile the applications became numerous and the system concepts have been adopted to the available technologies. Typical applications are speed control, air traffic control, synthetic aperture radar, airborne and spaceborne missions, military applications and remote sensing. Research for medical radar applications is well progressing for breast cancer detection and tumor localization. Automobile radar for save and autonomous driving are meanwhile produced in millions per year. In the next years the state-of-the-art radar system concepts will experience almost a revolution. Despite the significant advancements, the radar system technology did not develop like communications or other technologies during the last 20 years. Some of these new technologies will within a few years penetrate radar and revolutionize radar system concepts. This will then allow for new radar features and radar signal processing approaches.

Meinel, H. H. (2014). Evolving automotive radar - From the very beginnings into the future. In *8th European Conference on Antennas and Propagation* (EuCAP 2014), April 6-11, 2014, The Hague, The Netherlands, pp. 3107-3114.

Automatic cruise control (ACC) systems based on mm-wave radar have been under development for several decades… In the early 1970s the first test cars with 35 GHz sensors were road-tested. More than 20 years later in 1998 the Mercedes-Benz DISTRONIC system at - then - 77 GHz became operational. [Eight] years later this was followed by the DISTRONIC PLUS system going in series production for premium cars, combining a 77 GHz long range radar sensor (LRR) with two 24 GHz short range radar sensors (SRR) and making the system fit for urban traffic. Today this technology has moved to commercial stage with all major automotive manufacturers worldwide, lately introducing ACC systems also in the small car segment.

Li, J. Z.-C. (2014). *Design and signal processing for CMOS automotive radar* (Ph.D. thesis, University of Melbourne, Melbourne, AU)

> *There is an increasing use of radar for sensing the environment in automotive applications to provide data for applications such as collision avoidance and adaptive cruise control systems. In this thesis, the waveform design, signal processing and architecture of automotive radars are explored. A particular emphasis is placed on reducing the implementation cost to enable widespread adoption of safety systems. While an automotive radar is unlikely to experience intentional jamming, the anticipated increase in density of radars with falling cost and improved availability is expected to lead to more interference as more users begin to share the available band. It is thus important that the performance of the system is understood in the presence of interference. This thesis provides some insight into the severity of the problem and some strategies for mitigating the impact.*

Schipper, T., Mahler, T., Harter, M., Reichardt, L., & Zwick, T. (2013). An estimation of the operating range for frequency modulated radars in the presence of interference. In *2013 European Radar Conference (EuRAD)*, October 9-11, 2013, London, pp. 227-230.

> *This paper presents a basic model to estimate the operating distance of frequency modulated (FM) radars in the presence of FM interference. A function is provided to draw the equipotential lines for given S/I values in the frequency domain as a function of the spatial distribution of targets and interferers. The paper further includes a description of the gain versus deterministic interference. Conclusions are that smaller radar targets can be masked by other radars or that targets could mask themselves if they are equipped with a radar. The latter happens from a distance called Target Self-Masking Distance (TSMD).*

3.3 Testing and performance measures for radar in a congested environment

The research team in this study considers two types of tests important for the understanding of the impact of interference in the operation of radars in congested environments:

1. Validation of models used to estimate interference levels
2. Evaluation of mitigation strategies (i.e., automotive safety tests)

Experiments designed to address the first topic are needed because of the complicated propagation environments where automotive radars must operate. The research team from MTRI believes that experiments which validate existing models serve two purposes: validate the accuracy of the models, and develop empirical models for specific environments and scenarios. Such data may be collected with designed experiments, or measurements of systems operating "in the wild". While the current density of automotive radars is relatively low, measured data can be resampled to emulate conditions for evaluating systems intended to operate in congested environments.

Experiments designed to address the second topic, to evaluate mitigation strategies, are better represented in the literature, and are needed to ensure that the interference mitigation systems are effective and do not produce unsatisfactory side-effects. Much of the literature in this area follows the work pioneered by the MOSARIM study, which considers the use of a "norm-interferer" to produce the interference environment for evaluating individual systems.

Torres, F., Frank, C., Weidmann, W., Mahler, T., Schipper, T., & Zwick, T. (2012). The norm-interferer - an [sic] universal tool to validate 24 and 77 GHz band automotive radars. In *2012 9th European Radar Conference (EuRAD)*, October 29-November 2, 2012, Amsterdam, The Netherlands: pp. 9-12.

> *The European funding project MOSARIM (MOre Safety for All by Radar Interference Mitigation) started in January 2010 with the main objectives to investigate possible automotive radar interference mechanisms by both simulation and real-world road-tests and assess possible countermeasure and mitigation techniques in general guidelines and recommendations.*

Chauhan, R. (2014). *A platform for false data injection in frequency modulated continuous wave radar* (Master's degree dissertation, Utah State University, Logan, Utah).

> *[Radar] transmits radio waves in a known direction, which when intercepted by an obstruction/object are reflected by its surface and are received back at the radar system. The round trip delay time along with the known velocity of radio waves gives an accurate measurement of the distance of the object from the radar system. In a somewhat similar fashion, some radars are even capable of measuring the velocity of this object. Frequency-modulated continuous-wave (FMCW) radar is one such radar system, which is a subclass of continuous wave (CW) radars, where a continuous sinusoidal radio energy is transmitted, reflected, and received back at the radar system. These radar systems are widely used in vehicle automation technologies such as adaptive cruise control (ACC) and collision avoidance systems (CAS) to measure the distance from the nearest vehicles and maintain a safe following distance. But in designing these systems, little attention has been given to security, and these systems have vulnerabilities that are capable of compromising the whole purpose of making such systems.*

3.4 Mitigation techniques

Radar interference occurs when radars sharing a band overlap in time, space, frequency, polarization and modulation (coding). However, not all strategies are equal in cost, or effectiveness. The literature reveals great interest in modulation diversity, but this appears to be mostly academic. The industry relies largely on two modulation schemes: linear frequency modulated continuous wave (LFMCW) and frequency shift keying (FSK). There is interest in seeing linear polarized radars operate at a consistent rotation angle (clocking) of 45 degrees to reduce the interference experienced by radars in opposing traffic. This is shown in Figure 3. However, this is not regulated and there is little published on the topic. It also requires that all vehicle use the same polarization. The technique could reduce interference by 15 dB, subject to the environment.

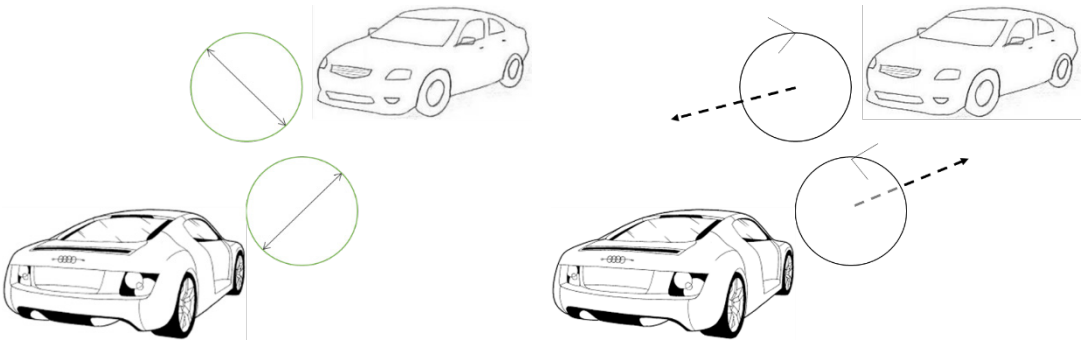

Figure 3: Vehicles traveling in opposite directions are shown. At left, linear polarized transmitters are 'clocked' at 45 degrees. At right, left-handed circularly polarized transmitters are employed, but the receive antennas are right-hand circular polarized to sense primary reflections.

The literature contains ideas for frequency diversity. There is some innovative work in use of orthogonal frequency division multiplexing access (OFDMA) transmission for simultaneous communications and radar functions. However, much of this is of interest to academics and possibly future systems, and does not seem to be in current automotive radar systems. The main frequency diversity technique, represented in literature and interviews with industry, is frequency hopping.

The principal tool for mitigating interference, found consistently in literature and interviews with industry, is the use of spatial diversity, in particular, digital beamforming. The idea is that the receiver can be focused narrowly in one direction, and reduce interference from other directions. Given an array antenna with several elements, this technique can mitigate interference by 10 to 20 dB.

3.4.1 **Spatial**

Gianelli, C., Li, J., & Stoica, P. (2015). *Coherent mimo radar and waveform diversity*. Wiley Encyclopedia of Electrical and Electronics Engineering: 1-19. doi.org/10.1002/047134608X.W8277

> *Multiple-input multiple-output (MIMO) radar technology has gained considerable attention, from both theorists and practitioners, in the past decade due to its capability to expand radar system functionality and open previously unexplored design space. This work seeks to provide a basic understanding of coherent MIMO radar technology, the performance enhancements that can be attained by using the technology, and the associated drawbacks involved in operating a coherent MIMO radar. Attention is paid to achieve the required waveform orthogonality for a MIMO radar system, and several operating concepts are presented and described.*

Bechter, J., Eid, K., Roos, F., & Waldschmidt, C. (2016). Digital beamforming to mitigate automotive radar interference. In *2016 IEEE MTT-S International Conference on Microwaves for Intelligent Mobility,* May 19-20, 2016, San Diego, CA.**:** pp. 1-4.

> *Interference between automotive radars decreases the sensors' detection capabilities. It is possible to use digital beamforming (DBF) in multi-antenna systems to reduce the power received from certain directions of arrival (DoA). If digital beamforming is used to mitigate the effect of an interferer, it is shown that it is not sufficient to cancel the*

DoA of an interferer alone, if an I-Q mixer is not present. Additionally, a second DoA must be blinded out. A DBF system which performs this task is presented. Experimental and simulated results support the mathematical derivation and show possible improvements with DBF.

Bourdoux, A., Ahmad, U., Guermandi, D., Brebels, S., Dewilde, A., & van Thillo, W. (2016). PMCW waveform and MIMO technique for a 79 GHz CMOS automotive radar. In *2016 IEEE Radar Conference*, May 2-6, 2016, Philadelphia**:** pp. 1-5. DOI: 10.1109/TVT.2014.2321175

Automotive radars in the 77-81 GHz band will be widely deployed in the coming years. This paper provides a comparison of the bi-phase modulated continuous wave (PMCW) and linear frequency-modulated continuous wave (FMCW) waveforms for these radars. The comparison covers performance, implementation and other non technical aspects. Multiple Input Multiple Output (MIMO) radars require perfectly orthogonal waveforms on the different transmit antennas, preferably transmitting simultaneously for fast illumination. In this paper, we propose two techniques: Outer code and Range domain, to enable MIMO processing on the PMCW radars. The proposed MIMO techniques are verified with both simulation and lab experiments, on a fully integrated deep-submicron CMOS integrated circuit designed for a 79 GHz PMCW radar. Our analysis shows that, although not widely used in the automotive industry, PMCW radars are advantageous for low cost, high volume single-chip production and excellent performance.

Dudek, M., Nasr, I., Bozsik, G., Hamouda, M., Kissinger, D., & Fischer, G. (2015). System analysis of a phased-array radar applying adaptive beam-control for future automotive safety applications. *IEEE Transactions on Vehicular Technology, 64*: 34-47.

In this contribution, we present a novel beam-control approach for automotive phased-array radar frontends. Since radar sensors are considered to be one of the means to enable future advanced safety functionality, we previously developed a system simulation environment that incorporates all involved domains and calculates all relevant high-level effects accurately. Subsequently, a generic phased-array FMCW radar frontend has been implemented and parameterized according to state-of-the-art SiGe components operating in the 77 GHz band. To demonstrate the advantages of an adaptively controlled beam for future safety applications, it is focused on curved traffic situations, which are calculated in a co-simulation incorporating a 3D-raytracer. A novel method for the control of the antenna characteristic is derived, which takes the specific curve geometry into account, and predictive enhancement features applied to it are elucidated, before their utilization and the resulting increase of system performance is computed. By adaptively coupling the radar sensor to the steering angle, thus directing its beam together with the ego-vehicle into the curve, its measurement range can be distinctly increased, which is providing more time for the safety system to react. This set of facts is first examined in a static view, by regarding only some specially selected time steps, before a thorough analysis of the complete traffic scenario reveals the system's advantages from a dynamic point-of-view. As a result, the performance improvement of phased-array frontends applying adaptive beam-control compared to those with body-fixed non-steerable beams is proven. Moreover, some results which are to be expected from such an advanced

system, in case its full potential is evolved by implementing a scanning functionality, are provided as an outlook on future developments.

Pfeffer, C., Feger, R., Wagner, C., & Stelzer, A. (2013). FMCW MIMO radar system for frequency-division multiple TX-beamforming. *IEEE Transactions on Microwave Theory and Techniques, 61*: 4262-4274.

In this paper, a prototype automotive radar sensor is presented that is capable of generating simultaneously multiple transmit (TX) beams. The system is based on a four-channel 77-GHz frequency-modulated continuous-wave (FMCW) radar system. The number of beams, their radiated power, steering angle, and beam pattern can be changed adaptively. This is achieved by the utilization of orthogonal waveforms applied to different beams in combination with digital beamforming on the receive side. Key components are vector modulators in the TX path controlled by digital-to-analog converters. The performance of the system is shown in measurements focused on beam pattern, signal-to-noise ratio, and susceptibility in case of interfering targets at cross-range. Measurement results are discussed and compared to theory and simulations. Furthermore, crest factor minimization of the vector modulator's control signals is introduced and used to increase the achievable TX power, which will be also shown in measurements.

3.4.2 **Temporal**

Choi, J.-H., Lee, H.-B., Choi, J.-W., & Kim, S.-C. (2016). Mutual interference suppression using clipping and weighted-envelope normalization for automotive FMCW radar systems. *IEICE TRANSACTIONS on Communications, E99-B*: 280-287.

With extensive use of automotive radars, mutual interference between radars has become a crucial issue, since it increases the noise floor in the frequency domain triggering frequent false alarms and unsafe decision. This paper introduces a mathematical model for a frequency-modulated continuous-wave (FMCW) radar in interfering environments. In addition, this paper proposes a time-domain interference suppression method to provide anti-interference capability regardless of the signal-to-interference ratio. Numerical results are presented to verify the performance of a 77GHz FMCW radar system with the proposed method in interference-rich environments.

3.4.3 **Spectral**

Li, X., Hu, Z., & Qiu, R. C. (2014). Demonstration of cognitive radar for target localization under interference. *IEEE Transactions on Aerospace and Electronic Systems, 50*: 2440-2455.

An ultra-wideband (UWB) multiple input/multiple output (MIMO) cognitive radar has been developed and demonstrated for the first time. Field-programmable gate array (FPGA) is used for waveform-level computing, while waveform optimization is accomplished in CPU. Working as a closed loop, convex optimization is applied to jointly design (arbitrary) transmitted waveforms and the receiving filters in response to the varying wireless environment. Multiple targets localization in the presence of interference is demonstrated. Shown in the experiment, performance improvement is obvious in all interference patterns.

Braun, K. M. (2014). OFDM radar algorithms in mobile communication networks (Doctoral dissertation, Karlsruher Instituts für Technologie, Karlsruhe, Germany).

> *Radar systems have changed in a similar way to mobile communications. What once used to be expensive technology, restricted to a limited circle of users, has become accessible to anyone. Radar sensors have become cheaper, less power-consuming and can be found in many different applications, ranging from industrial automation to consumer products such as automobiles. Many of these applications also require communication capabilities, and given the similarities between the nature of wireless data transmission and radar – both emit and receive electromagnetic waves – it is an obvious question to ask if both components could be combined into a single device. Such a combined system would require less hardware, less power and allocate less spectrum – all of these characteristics being highly desirable in mass-produced technology.*
>
> *All results are verified with simulations and some measurements, all of which suggest high applicability of OFDM for combined radar and communication systems.*

Roberton, M., & Brown, E. R. (2003). Integrated radar and communications based on chirped spread-spectrum techniques. *IEEE MTT-S International Microwave Symposium Digest, 1*: 611-614.

> *Linear frequency modulated (LFM) signals and the associated pulse compression techniques are attractive in applications where highly secure and robust communication is needed. This paper investigates the novel integration of radar and communications utilizing LFM waveforms. The simulations suggest that the performance of the communications-receiver deviates at most 2 dB from the theoretical probability of bit error for $\pi/4$-differential phase shift keying. The simulated radar receiver-operating characteristics for false-alarm probabilities between 10-2 and 10-4 also compares very well with the theoretical limits for a coherent system.*

Luo, T. N., et al. (2013). A 77-GHz CMOS automotive radar transceiver with anti-interference function. *IEEE Transactions on Circuits and Systems I: Regular Papers, 60*: 3247-3255.

> *This paper presents a 77-GHz long-range automotive radar transceiver with the function of reducing mutual interference. The proposed frequency-hopping random chirp FMCW technique reconfigures the chirp sweep frequency and time every cycle to result in noise-like frequency response for mutual interference after the received signal is down-converted and demodulated. Thus, the false alarm rate can be reduced significantly. The transceiver IC is fully integrated in TSMC 1P9M 65-nm digital CMOS technology. The chip including pads occupies a silicon area of 1.03 mm × 0.94 mm. The transceiver consumes totally 275 mW of power, and the measured transmitting power and receiver noise figure are 6.4 dBm and 14.8 dB, respectively. To the authors' knowledge, this is the first integrated 77-GHz automotive radar transceiver with the feature of anti-interference.*

Gerlach, K. (1998). Thinned spectrum ultrawideband waveforms using stepped-frequency polyphase codes. *IEEE Transactions on Aerospace and Electronic Systems, 34*: 1356-1361.

> *An ultrawideband (UWB) radar can interfere with external RF sources because of the mutual occupancy of the same frequency band. A stepped-frequency polyphase code (SFPC) waveform is proposed as a generic UWB waveform whose interference with the external RF sources is significantly reduced. The subpulses of the individual stepped-frequency (SF) pulses are phase coded using small phase perturbations. This results in a waveform which places nulls at the frequency locations of the external RF sources. Because the phase perturbations are small, a mismatched filter which uses the unperturbed pulses (no phase modulation) as a reference signal results in a simple receiver design and a small mismatch loss on receive. Furthermore, the proposed methodology also has application to narrowband or wideband radars.*

3.4.4 **Coding**

Galati, G., & Pavan, G. (2013). Noise radar technology as an interference prevention method. *Journal of Environmental Chemical Engineering*: *4*:4-4:4.

> *In some applications, such as automotive and marine/navigation, hundreds of radars may operate in a small environment (e.g., a road complex or a strait) and in an allocated frequency band with limited width. Therefore, a compatibility problem between different radars arises that is not easily solved by time, frequency, space, or polarization diversity. The advent of fast digital signal processing and signal generation techniques makes it possible to use waveform diversity to solve this problem that will be exacerbated in the next future. Ideal waveforms for the diversity are supplied by Noise Radar Technology (NRT), whose application is promising in some military applications as well as in the civilian applications considered in this paper. In addition to being orthogonal as much as possible, the random signals to be transmitted have to satisfy requirements concerning side lobe level and crest factor, calling for novel, original design and generation processes.*

Lee, H.-B., et al. (2016). *Interference mitigation by high-resolution frequency estimation method for automotive radar systems*. *The Journal of Korean Institute of Communications and Information Sciences 41*: 254-262.

> *With the increased demand for automotive radar systems, mutual interference between vehicles has become a crucial issue that must be resolved to ensure better automotive safety. Mutual interference between frequency modulated continuous waveform (FMCW) radar system appears in the form of increased noise levels in the frequency domain and results in a failure to separate the target object from interferers. The traditional fast Fourier transform (FFT) algorithm, which is used to estimate the beat frequency, is vulnerable in interference-limited automotive radar environments. In order to overcome this drawback, we propose a high-resolution frequency estimation technique for use in interference environments. To verify the performance of the proposed algorithms, a 77GHz FMCW radar system is considered. The proposed method employs a high-resolution algorithm, specially the multiple*

signal classification and estimation of signal parameters via rotational invariance techniques, which are able to estimate beat frequency accurately.

Martone, A., McNamara, D., Mazzaro, G., & Hedden, A. (2013, January). *Cognitive nonlinear radar* (Report No. ARL-MR-0837). Adelphi, MD: Army Research Laboratory.

In this report, a unique cognitive nonlinear radar (CNR) is introduced. Research and development efforts for the CNR are currently funded by the U.S. Army Research Laboratory (ARL). The CNR adapts to (1) an increasingly cluttered electromagnetic (EM) environment, a growing problem for ground-based and airborne radar systems; (2) multiple targets; and (3) other radar, communication, and electronic systems that must operate without interfering with each other. The CNR uses a narrowband, nonlinear radar target detection methodology. This methodology has the advantage, as compared with other nonlinear radar systems that do not implement a cognitive scheme, to adapt to the radio frequency (RF) environment by intelligently selecting waveform parameters using adaptive algorithms. The adaptive algorithms optimize the waveform parameters based on (1) the EM interference, (2) target likelihood, and (3) permissible transmit frequencies as specified by regulations and allowable by other systems operations within the environment.

Leshem, A., Naparstek, O., & Nehorai, A. (2007). Information theoretic adaptive radar waveform design for multiple extended targets. *IEEE Journal of Selected Topics in Signal Processing, 1*: 42-55.

In this paper, we use an information theoretic approach to design radar waveforms suitable for simultaneously estimating and tracking parameters of multiple extended targets. Our approach generalizes the information theoretic water-filling approach of Bell to allow optimization for multiple targets simultaneously. Our paper has three main contributions. First, we present a new information theoretic design criterion for a single transmit waveform using a weighted linear sum of the mutual information between target radar signatures and the corresponding received beams (given the transmitted waveforms). We provide a family of design criteria that weight the various targets according to priorities. Then, we generalize the information theoretic design criterion for designing multiple waveforms under a joint power constraint when beamforming is used both at the transmitter and the receiver. Finally, we provide a highly efficient algorithm for optimizing the transmitted waveforms in the cases of single waveform and multiple waveforms. We also provide simulated experiments of both algorithms based on real targets and comment on the generalization of the proposed technique for other design criteria, e.g., the linearly weighted non-causal MMSE design criterion.

Mu, L., Xiangqian, T., Ming, S., & lun, Y. (2009). *Research on key technologies for collision avoidance automotive radar*. 2009 IEEE Intelligent Vehicles Symposium, Xi'an, China, June 3-5, 2009, pp. 233-236.

Anti-interference capability and low cost play decisive roles for the break-through on the market of collision avoidance automotive radar. With the increasing use of automotive radar, the mutual interference becomes an issue. This paper proposes a novel signal design and signal processing methods for automotive radar, which combine good anti-interference capacity and the low cost of conventional frequency

modulated continuous wave (FMCW) radar. The radar signal is easy to be generated and its signal processing can be performed by Fast Fourier Transform (FFT) algorithm. So, the proposed new methods [are] feasible and effective.

Song, X., Zhou, S., & Willett, P. (2010). Reducing the waveform cross correlation of MIMO radar with space-time coding. *IEEE Transactions on Signal Processing, 58*: 4213-4224.

Multiple-input-multiple-output (MIMO) radar is attractive for target detection, parameter identification, and target classification due to diversity of waveform and perspective. However, the mutual interference among the waveforms may lead to performance degradation in resolving spatially close returns. In this paper, we consider the use of space-time coding (STC) to mitigate the waveform cross-correlation effects in MIMO radar. First, it turns out that a joint waveform optimization problem can be decoupled into a set of individual waveform design problems. Second, a number of monostatic waveforms can be directly used in a MIMO radar system, which offers flexibility in waveform selection. We provide conditions for the elimination of waveform cross correlation, and discuss four kinds of space time codes. In addition, we also extend the model to partial waveform cross-correlation removal based on waveform set division. Numerical results demonstrate the effectiveness of STC in MIMO radar for waveform decorrelation.

Thayaparan, T., Dakovic, M., & Stankovic, L. (2008). Mutual interference and low probability of interception capabilities of noise radar. *Sonar Navigation IET Radar 2*: 294-305.

Recently, there has been considerable interest in noise radar over a wide spectrum of applications, such as through-wall surveillance, tracking, Doppler estimation, polarimetry, interferometry, ground penetrating or subsurface profiling, detection, synthetic aperture radar (SAR) imaging, inverse SAR imaging, foliage penetration imaging etc. Major advantages of using noise in the transmit signal are its inherent immunity from radio frequency and electromagnetic interference, improved spectrum efficiency, and hostile jamming as well as being very difficult to detect.

4 Interviews with Automakers and Suppliers

"We do not see a problem [with mutual interference of radars] at this time, but we know it will be." -Tom Wilson, ADAS Product Line Manager, NXP Semiconductors, N. V. (Eindhoven, The Netherlands), at ADAS and Autonomy Vehicles USA Conference, Novi, MI, October 16-17, 2016

The radar congestion study conducted a series of interviews with automobile makers and automotive radar manufacturers. The interviews were conducted under the title "The Future of Automotive Safety Sensors." They gathered information on the trends in automotive safety sensor to understand the current technologies integrated into automotive radar systems, and their roles in advanced safety and assisted driving technologies. The study sought each manufacturers' view of the future of these systems and how these systems operate in congested scenarios.

The interviews were designed to explore the range of radar architecture options being deployed to help understand their strengths and vulnerabilities in regard to interference; as well as, obtain the manufacturers' assessment of projected deployment level for the future, risk of interference, and the technology developments that may mitigate the impact of interference.

4.1 Industry use of radar

Automotive companies were asked about the use of sensors in the development of new cars. They report two main reasons to push forward with adopting sensors for active safety.

1. To support driving assistance features, such as collision avoidance warning and automated emergency breaking
2. Vehicle autonomy: Automakers and suppliers want to be positioned as leaders in mobility.

The automakers consider radar an important contributing sensor for meeting new safety requirements and developing autonomous vehicles.

4.2 Recognition of threat posed by mutual interference

Automakers and suppliers understand that mutual interference is a potential problem with varying levels of concern. While aware of the potential for degraded performance, they report only limited testing. There is a recognition, though, that this will grow as an area of concern with greater levels of deployment.

In general, the radar manufacturers and automakers are optimistic that the industry will be able to make use of automotive radars and mitigate the impact of interference for congested operation. Methods for managing and mitigating problems with mutual interference identified in discussions are as follows.

- Consortium of suppliers
- Technology convergence over time
- Cross-licensing the best technologies
- Complementarity of sensors
- Individual companies designing the technology so no matter what situation, their technology works
- FCC for harmonizing common strategies and common solutions

4.3 System response to interference

At a high level, the system must operate whether a sensor is suffering from interference or not. The automakers and system suppliers respond to the degradation of radar performance due to radio-frequency interference (RFI) in multiple ways. It is important to realize that the industry is still working to increase acceptance of this technology, while wanting the public to understand that the systems are at Level 1 and 2 autonomy, see Table 3, in which the human driver is always expected to monitor the driving performance, and be prepared to take over all dynamic driving tasks should the autonomous systems fail.

Table 3: SAE Autonomy Levels

SAE level	Name	Execution of Steering and Acceleration/ Deceleration	*Monitoring* of Driving Environment	Fallback Performance of *Dynamic Driving Task*	System Capability *(Driving Modes)*
Human driver monitors the driving environment					
0	No Automation	Human driver	Human driver	Human driver	n/a
1	Driver Assistance	Human driver and system	Human driver	Human driver	Some driving modes
2	Partial Automation	System	Human driver	Human driver	Some driving modes
Automated driving system ("system") monitors the driving environment					
3	Conditional Automation	System	System	Human driver	Some driving modes
4	High Automation	System	System	System	Some driving modes
5	Full Automation	System	System	System	All driving modes

Based on the interviews with automobile makers and automotive radar manufacturers the team finds that the advanced driver assist systems response to mutual interference may involve RFI mitigation techniques, or not, as discussed in Table 4.

Table 4: Techniques used by automotive manufacturers and suppliers to either mitigate or avoid RFI.

	RFI mitigation techniques	Avoidance techniques that do not require RFI mitigation
RF pulse collisions	• Pulse to pulse processing - remove polluted pulses	• Reduce sensitivity of detection algorithms (CFAR approach) • This results in degraded performance
Spectrum occupied	• Sniff and avoid • Frequency diversity	• Disable sensor supported feature and notify driver

Congested environment	• Spatial processing (not adaptive)
	  • Narrow main-beam
	  • Side-lobe null steering
		• Shift function to a different sensor
		• Operate using tactic not dependent on radar

4.4 Tests

Respondents suggest that limited testing is being done in the following areas:

- Limited testing of interference from radars of the same brand (intra-manufacturer): Typically, this is used to ensure that multiple radars operating on a single car do not electrically interfere with one another.

- Limited testing of interference from radars of the competing brands (inter-manufacturer): Manufacturers are conducting experiments to ensure that there are no detrimental effects from operating in proximity to other manufacturers systems. However, these tests focus on a few, major providers of hardware, and testing is typically limited to one-on-one interactions in limited scenarios.
- Some realize own systems are vulnerable: Some of the manufacturers explain that their hardware can suffer if operating in proximity to similar units. This is understood as a problem that must be dealt with at the system level.
- Automakers rely largely on testing by suppliers: The automakers do not typically test for interference, but assume that this is tested by the radar manufacturers.

4.5 Trends

In discussing future trends, the industry is understandably protective about this topic, however, some themes were consistently brought up.

- System on chip processing: Radar signal processing will be performed in hardware, referred to as system on chip processing, rather than relying on more general purpose processing units. This results in faster operation, reduced packaging size, and reduces the cost of implementing sophisticated digital signal processing.
- Digital beam-forming: This is referred to as 3D scanning and holographic radar in the industry. A digital beamforming receiver is related to an electronically steered receiver array, shown in Figure 4. However, an electronically steered array is used to sweep out a pattern, by changing the electronic delays used to cohere the radio frequency energy incident on the antenna elements, in angle; whereas, in a digital beamforming receiver must digitize and store the received signals from each antenna element, and perform the angular coherent processing on the stored data. The transmitter illuminates a large field of view (FOV), which is processed into multiple narrow beams, the instantaneous field of view (IFOV) in the receiver. The entire system can be physically swept over a larger field of regard (FOR).

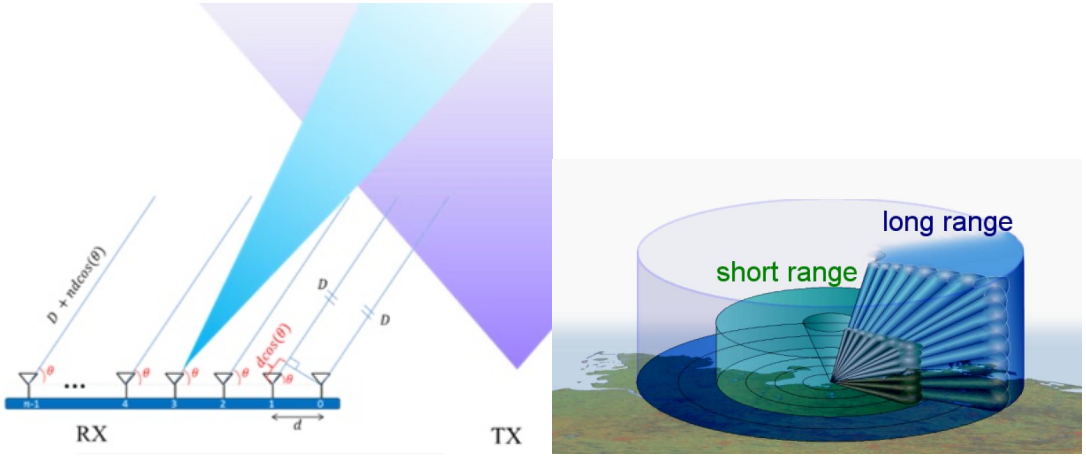

Figure 4: At left, delays introduced across the receiving antenna elements focus the directional response of the radar, in an electronically steered array (ESA) receiver. At right, is a graphic showing the response of a digital beamforming radar system.

- Digital Modulation Radar: The use of digital modulation to allow for coded waveforms that can reduce interference was mentioned by one manufacturer. Interviewees see this as a future development, if needed.

Understanding that systems may employ numerous cameras, radars, and lidars, the interviewees were asked to comment on the role fusion (combining information from more than one sensor) may play in driver assist systems. The following advantages were identified.

- Improved safety performance by reducing the risk for single point of failure
- Interference mitigation:
    - System redundancy
    - Cross-validation for sensor reports through voting

Engineers in the industry understand and report that sensor fusion adds complexity and requires greater processing speed and must not allow network latency to introduce unacceptable lags in decision times.

4.6 Interview process

Interviewees were selected from major developers and integrators of automotive radar, and their willingness to participate. The interviews were conducted from January to March 2017. The study was limited to nine industry representatives. Companies with complete interviews include:

- Manufacturers: Fiat-Chrysler, Ford, and General Motors; and
- Suppliers: Bosch, Denso, Magna, NPX, Valeo, and ZF/TRW.

The interviewees were provided advance copies of the questions. Participants were invited to interview in person, or by telephone. In person interviews were conducted at the University of Michigan Transportation Research Institute, or at interviewee's choice of location. Additionally, automotive device supplier, Delphi, is a partner organization on the research team, and provided additional detail on industry practices and current technologies.

Interviews were led by Bruce Belzowski of the University of Michigan's Transportation Research Institute. Belzowski has authored and co-authored research reports focusing on a variety of topics including the deployment of safety technologies, interoperability issues for commercial safety applications, the potential benefits of larger trucks, and the current use and benefits of onboard safety technologies.

The interviews were assisted and assessed by the following subject matter experts in radar and electronic warfare (EW) from Michigan Tech Research Institute: Nikola Subotic has 30 years of experience in the advancement of synthetic aperture radar and electro-optical systems; William Buller has 20 years of experience in radar system design, performance characterization, target modeling, and algorithm development for radar and EW; and Brian Wilson has 10 years of experience designing, developing and experimenting with radar and software defined radio

5 Models for Estimating Interference

5.1 Radar models

For the purposes of modeling and simulation, a generic class of radar sensor parameters have been established, based on values selected from radar specifications and refined by review of experts at two principal automotive radar manufacturers. The resulting parameters are shown in Table 5.

Table 5: Parameters used for generic radar to model interference level.

	Long Range Radar	**Medium Range Radar**	**Short Range Radar**	**Units**
Mean Transmitter Power $\bar{P}_S$	1	0.3	0.1	watts
Reference Target (Range, RCS)	$100, 0$ (175, 10)	50, 0 (88, 10)	20, 0 (35, 10)	(meters, dBm^2)
Transmitter Bandwidth B_{TX}	200	400	500	MHz
Range Resolution $\left(\frac{c}{2\,B_{TX}}\right)$	0.75	0.375	0.3	meters
Range Bins	200	200	60	#
Compression Gain	23	23	18	dB
Carrier Frequency	76-77 76-81	76-77 76-81	76-77 76-81	GHz GHz
Noise Factor, f_N	10	10	10	ratio
Duty Factor DF	0.5	0.9	1	ratio
FOV θ Azimuth	20	90	150	degrees
FOV θ Elevation	5	10	10	degrees
Antenna Gain	27	20	17	dB
Azimuth Resolution	5	15	50	degrees
Range Rate Limits	[-100 100]	[-100 100]	[-100 100]	meters / second

Table 6: Description of radar parameters

PARAMETER	MEANING
Mean Transmitter Power $\overline{P}_S$	The average power radiated by the transmitting antenna
Reference Range and Target	Target's radar cross-section (reflection strength) at which radar achieves desired detection probability specified at a given distance (reference range)
Transmitter Bandwidth	The total spectrum spanned by the transmitter
Range Resolution	Forward distance required between two point targets to resolve into two detections
Range bins	Discrete samples in time are converted to range bins
Compression gain	The net gain in power resulting from isolating a target's power in range
Carrier Frequency	Frequency of the RF carrier
Noise Factor	The ratio of the system output noise relative to thermal background noise.
Duty Factor	The ratio of time in which the system transmits
FOV θ Azimuth	Angular width of area within main-beam of radar in horizontal direction
FOV θ Elevation	Angular height of area within main-beam of radar in vertical direction
Azimuth Resolution	Horizontal angle required between two point targets to resolve into two detections
Range Rate Limits	Minimum and maximum detectable per-second change in relative range between ego vehicle and target

5.2 Interference model

How much power does a given radar receive from other radar transmitters?

The question is answered by developing a model for nominal automotive radars and computing the amount of power overlapping in space, time, and spectrum. The overlap in time and spectrum are computed directly from the radar parameters, and the spatial component depends on the relative geometry of the radars participating in the scenario. This is computed stochastically.

Using parameters for a generic radar, summarized in Table 5, we can compute the expected interference level by computing the probability of intercept (POI) in spectrum, time, and space.

An assumption must be made about how the radar carrier frequency and pulse scheduling are selected. Three choices are described below, which bound the problem.

- the radars all use the same carrier frequency and are synchronized in time – this assumption would *maximize* the interference but is unrealistic.
- the radars cooperate to optimally avoid one another's transmissions – this assumption would *minimize* interference, but requires RF agility, which is not typical.
- the choice of center frequency is randomly selected in band, and no synchronization between systems – this assumption generates a moderate estimate of interference and is most realistic based on interview responses.

Based on the responses from interviewees, our understanding of the industry, and operation of units in production, the probability of intercept, POI, is based on the assumption that the choice of center frequency is selected randomly, uniformly distributed, in band, and there is no synchronization between systems.

This gives us the statistical model to compute the temporal and spectral POI, for each interferer-ego pair of radars. The interference is mutual, but the impacts are measured at one of the pair, which is termed the ego.

The spectral POI for a pair of radar is based on the amount of the available band they occupy, or channel fraction, CF. That is, a 200 MHz system, operating in the 76-to 77 GHz band, has a channel fraction of 0.2. The general equation for spectral POI in a population of K radars, ω_K, is shown below.

$$\omega_K = 1 - \prod_{k=1}^{K-1}(1 - CF_k)$$

Similarly, the temporal POI for a pair of radar is based on the amount of the available time they transmit, or duty factor, DF. The general equation for spectral POI in a population of K radars, T_K is shown below.

$$\mathrm{T}_K = 1 - \prod_{k=1}^{K-1}(1 - DF_k)$$

The total system overlap ξ_K, is the product of the temporal and spectral POI.

$$\xi_K = \omega_K \mathrm{T}_K$$

This overlap factor will be used in our interference estimation, which includes the transmitted power and antenna patterns, into a stochastic geometric model. The geometric model computes the mean interference, so the overlap is taken to be the pair-wise overlap. In this study, the pair-wise spectral overlap, ω_2 and temporal overlap T_2, reduce to CF_1 and DF_1, which are the channel fraction and duty factor, respectively, of the victim radar. The product of these, ξ_2, is the pair-wise overlap used in the interference model

We apply the stochastic geometric methods used to study interference in large random wireless networks (Al-Hourani, Evans, Kandeepan, Moran, & Eltom, 2017) to gain some insights. The method begins by modeling the interfering transmitters at-large as a *point process*, a way of modeling a random set. There are several varieties of point processes, but we will use a simple and natural process, the *Poisson point process.* It has a single parameter, λ, called the *intensity,* which is the average density of points in an interval. In our context, modeling interferers with a Poisson point process, Θ, with intensity $\lambda = 1/25$ m would mean that there is, on average, an interfering car every 25 meters along a road. An example distribution of vehicles under such a process, is shown in Figure 5.

Figure 5: Locations of vehicles are shown, distributed along a line, with a Poisson point process density of 1/25 meters.

From here, the quantity of interest is the cumulated interference I at a point y from all interfering nodes in the Poisson point process Θ,

$$I(y) = \sum_{x \in \Theta} P_x h_x l(|y - x|_2).$$

Here, P_x denotes the power received from the transmitter at x, h_x denotes the (random) power fading coefficient, and l denotes the path loss, which is assumed only to be a function of the distance between y and x. We will assume that $\mathbb{E}[h_x] = 1$.

Next, because we are using a Poisson point process, we can use Campbell's Theorem (Haenngi & Ganti, 2008) to calculate the mean of $I(y)$ with respect to the point process:

$$\mathbb{E}_\Theta[I(y)] = \mathbb{E}_\Theta\left[\sum_{x \in \Theta} P_x h_x l(|y - x|_2)\right] = \lambda\, \mathbb{E}[h_x] \int P_x l(|y - x|_2)\, dx = \lambda \int P_x l(|y - x|_2)\, dx.$$

From here, we need only adjust P_x and l to each scenario's geometry to compute the interference power. The following sections detail the application of the stochastic geometric model for each of the scenarios.

The interference levels are then used to modify the noise level in an automotive radar simulation, using Matlab's ADAS toolbox, described in Section 5.3 System model.

5.2.1 **Interference from opposing traffic**

In this scenario, we model the stochastic interference being caused by interfering cars in an opposing lane of traffic on a straight two-way road, as shown in Figure 6, below. Ego radar is on blue car and the interferers are the yellow cars in the opposing lane.

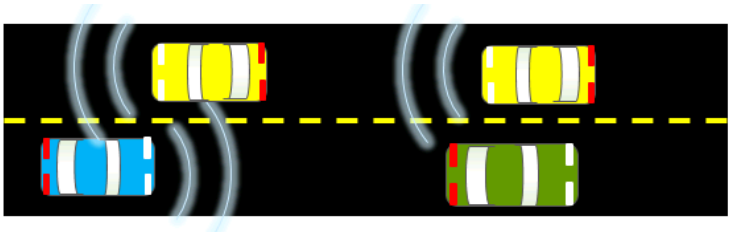

Figure 6: Scenario 1 is represented schematically above. The ego vehicle, in blue, operates a forward-looking radar, following a target vehicle, in green. The ego vehicle suffers from the operation of radars, which serve to interfere, in yellow, by opposing traffic.

This has a straightforward model for the received incident power, as it is direct path. Following the derivation from (Al-Hourani, Evans, Kandeepan, Moran, & Eltom, 2017), and assuming ego and interfering radars are identical and with the ego radar centered at the origin,

$$I_1 = \xi\lambda \int_{\delta}^{\infty} \frac{P_0\gamma_1}{L^2 + r^2} dr = \frac{\xi_2 S\lambda P_0\gamma_1}{L}\left(\frac{\pi}{2} - \arctan(\delta/L)\right),$$

where λ is the mean interferer density, P_0 is the transmitter power, ξ is the time-frequency overlap factor that accounts for the probability of collision, and $\delta = L/\tan(\theta/2)$ is the minimum distance away from the ego radar an interferer with FOV θ must be to illuminate the ego receiver. Finally, $\gamma_1 = {G_t}^2\left(\frac{c}{4\pi f}\right)^2$, where G_t and f refer to the antenna gain and operating frequency of the radar, respectively.

Table 7: Evaluating the constants for calculating the interference based on the radar parameters in Table 5.

Constant	Value LRR	Value MRR	Value SRR	Explanation
$\boldsymbol{P_0}$	1.0 W	0.3 W	0.1 W	Transmit power
$\boldsymbol{G_t}$	$\frac{16}{\sin(20°)\sin(5°)} = 27\ dB$	$\frac{16}{\sin(90°)\sin(10°)} = 20\ dB$	$\frac{16}{\sin(150°)\sin(10°)} = 17\ dB$	Antenna gain using elliptical beam based on FOV azimuth and elevation
$\boldsymbol{L}$	3.7 m	3.7 m	3.7 m	Lane width (U.S. standard)
$\boldsymbol{\delta}$	$\frac{L}{\tan\left(\frac{20°}{2}\right)} = 21$ m	$\frac{L}{\tan\left(\frac{90°}{2}\right)}$ =3.7 m	$\frac{L}{\tan\left(\frac{150°}{2}\right)}$ =3.7 m	Minimum distance from to interferer opposing lane to be illuminated

Given $\lambda = 1/x$, where x is the mean spacing of interferers, the interference levels, using the overlap ratio for the 76-77 GHz band are:

$$I_{1,LRR} = \frac{1.32 \times 10^{-4}\ (W \cdot m)}{x} \qquad I_{1,MRR} = \frac{2.23 \times 10^{-5}(W \cdot m)}{x}.$$

5.2.2 Interference from passing traffic

In this scenario, we wish to model the stochastic interference being caused by interfering cars in an adjacent, same-direction lane of traffic on a straight road as the ego (blue) approaches a target car (green), as shown below. As in the previous figure, the interferers are yellow.

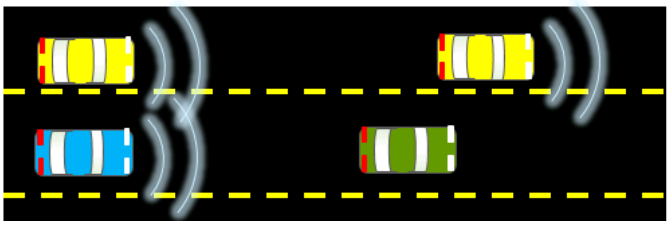

Figure 7: Scenario 2 is represented schematically above. The ego vehicle, in blue, operates a forward-looking radar, following a target vehicle, in green. The ego vehicle suffers from the operation of radars by other vehicles, yellow, in the adjacent lanes illuminating the same target.

This computation is similar to 4.1 but it has an extra constant to account for the reflection off the target. Note that this result will be a function of two parameters, mean interferer density and range to target.

$$I_2 = \xi\lambda \int_{\delta}^{\infty} \frac{P_0\gamma_1\gamma_2}{R^2(L^2+r^2)}\,dr = \frac{\xi_2\lambda P_0\gamma_1\gamma_2}{R^2 L}\left(\frac{\pi}{2} - \arctan(\delta/L)\right),$$

where R is the range to the target car, $\gamma_2 = \sigma_c/4\pi$ and σ_c is the radar cross section of the target, and the remaining parameters as in Table 7.

Again, using the parameters as summarized in Table 7, and $\sigma_c = 10$ m, we can compute I_2. Letting $\lambda = 1/x$ as before, we get the following scenario interference levels

$$I_{2,LRR} = \frac{2.84\times10^{-4}\ (W\cdot m)}{R^2 x} \qquad I_{2,MRR} = \frac{2.65\times10^{-5}\ (W\cdot m)}{R^2 x}.$$

5.2.3 **Interference while backing out of parking space**

In this scenario, we model the interference the rear-looking short-range radar experiences while backing out of a parking space that is perpendicular to the road, as shown below.

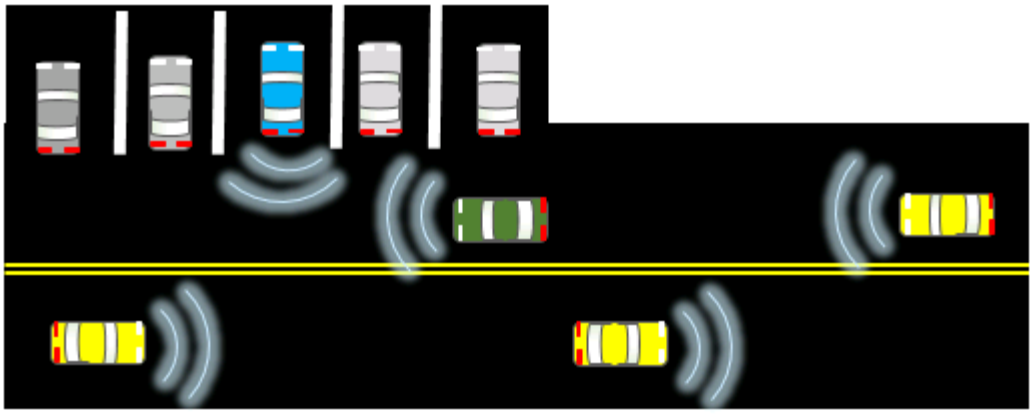

This scenario is very similar to 6.2, as the interference is all direct path. However, the different FOV arrangements must be taken into consideration. To begin, the FOVs of the SRR (150°) and the LRR (20°) are non-overlapping, so we will only consider side-lobe power levels in the integrand. For the MRR's FOV (90°), we have some more complicated geometry, as shown below.

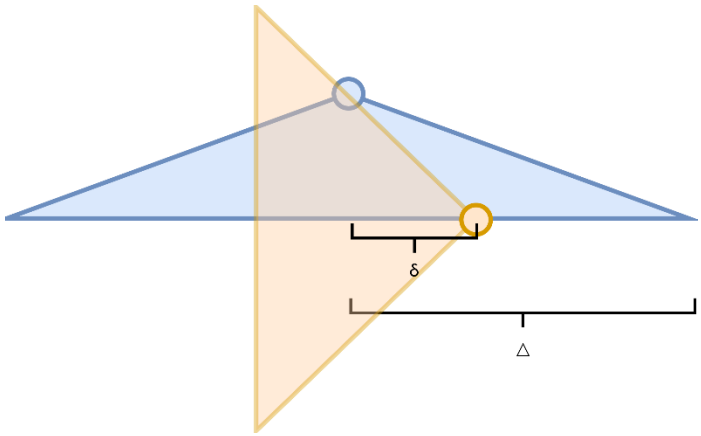

Figure 8: Ego rear-facing SRR (blue) receiver FOV overlapping with interferer MRR (orange) transmitter FOV.

For this regime, our integral calculation will be split in two – one part where the ego is illuminated with main lobe interference and can see it, i.e., when the interferer is on the interval between δ and Δ away, in the along-the-road sense. The other is when the main lobe of the interferer is illuminating the ego, but only in a receiver side-lobe. Here, $\Delta = L\tan\frac{\theta}{2}$ and δ is as in the previous section.

For both the LRR calculation and the MRR calculation we will assume a 10 dB down side-lobe for simplicity, but it is easy to adjust the calculation. Furthermore, both the MRR and LRR cases must repeated with another lane of traffic in the opposing direction, which will give us integrands with $(2L)^2$ and adjusted limits.

For the LRR situation, we get

$$I_{3,LRR} = \xi\lambda\left(\int_{\delta}^{\infty}\frac{\gamma_1 P/10}{r^2+L^2}\,dr + \int_{2\delta}^{\infty}\frac{\gamma_1 P/10}{r^2+(2L)^2}\,dr\right) = \frac{3P\gamma_1\lambda\xi_2\left(\pi - 2\arctan\left(\frac{\delta}{L}\right)\right)}{40L}.$$

For the MRR, there are four terms, a main lobe and a side-lobe term for each lane of traffic:

$$I_{3,MRR} = \xi\lambda\left(\int_{\delta}^{\Delta}\frac{\gamma_1 P}{r^2+L^2}\,dr + \int_{\Delta}^{\infty}\frac{\gamma_1 P/10}{r^2+L^2}\,dr + \int_{2\delta}^{2\Delta}\frac{\gamma_1 P}{r^2+(2L)^2}\,dr + \int_{2\Delta}^{\infty}\frac{\gamma_1 P/10}{r^2+(2L)^2}\,dr\right)$$
$$= \frac{3P\gamma_1\lambda\xi_2\left(\pi - 20\arctan\left(\frac{\delta}{L}\right) + 18\arctan\left(\frac{\delta}{L}\right)\right)}{40L}.$$

Using the constants from each radar and letting $\lambda = 1/x$ as before, we get the following functions

$$I_{3,LRR} = \frac{1.19\times10^{-4}\ (W\cdot m)}{x} \qquad I_{3,MRR} = \frac{4.14\times10^{-5}\ (W\cdot m)}{x},$$

which shows that the interference levels are nearly identical. If we assume that the SRR will be interfered by both an MRR and an LRR for each interfering vehicle, then $I_3 = I_{3,LRR} + I_{3,MRR} \approx 2\,I_{3,LRR}$, which may be a simpler approximation.

5.3 System model

To estimate the impact of interference on a collision warning system, the study introduces the interference powers, calculated as in the preceding sections, and models the interfering transmissions as uncorrelated noise. This approach is common in past studies (John & Schipper, 2012; Heuel, 2016; Al-Hourani, Evans, Kandeepan, Moran, & Eltom, 2017), and assumes the waveforms of the interfering radar are substantially different, so that their mutual energy does not correlate. Analysis of specific interactions for combinations of waveforms in automotive radar warrants further research, but requires a combinatoric analysis. The set of possible variations in waveform settings is large, and their impact is strongly dependent on the specifics of the signal processing chain behind the receiving radar's front end. While treating the interference as noise neglects the possible impacts of interfering signals, which generate false tracks (ghost targets), the impact is independent of hardware architecture. Thus, making the analysis here, more generally applicable.

To quantify possible system impacts, the processing functions are based on a generic model developed in cooperation with industry professionals and simulated in Matlab's Automated Driving System Toolbox. The approach can be adapted for higher fidelity models, with the specific signal processing chain for a particular brand and model of radar. However, in this study, the system model is only intended to demonstrate the impact on a generic, but reasonable, radar system that can be reproduced by other researchers with access to the ADAS Toolbox. The current study does not capture those system impacts, which depend on the multitude of interactions, which result from cross-correlation of different waveforms. This deficit deserves attention through further analysis, and, especially, with empirical tests.

To model a vehicle with advanced driver assistance sensors, it is necessary to be able to instantiate, manipulate, and support interactions between the various components within the scenario. This includes the following.

- Driving scenario generation, including:
    - Roadway definition
    - Definition of scene actors, including pedestrians and vehicles
    - Motion of those actors within the scene
- Definition and placement of desired sensors on the vehicles
- A sensor detection modeling environment
- Support for combining detections into tracks
- The ability to extract per-time-step information relating to vehicle positions, and detection and track information
- The ability to modify on a per-time-step basis the detector responses based on changing scene conditions
- Visualizations, including bird's-eye-view plots of sensor coverage, detections, and video overlays for lane markers

For our simulations, we implemented the processing flow in Figure 9:

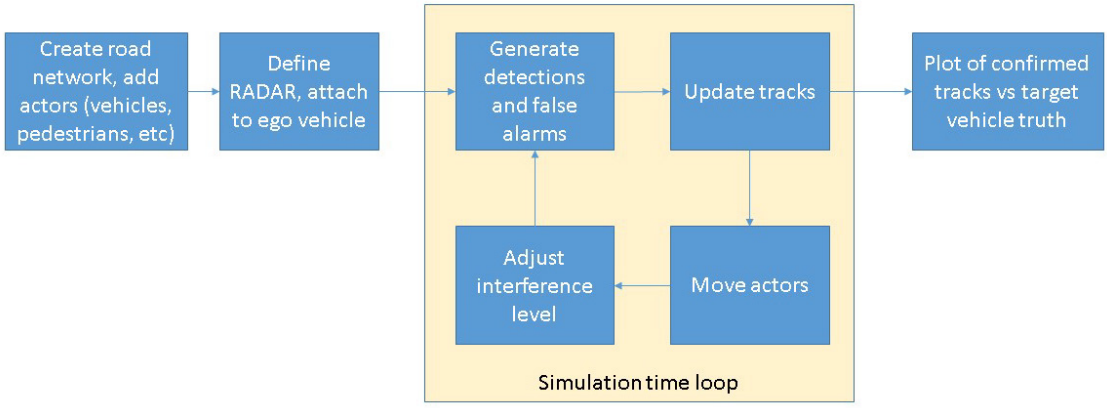

Figure 9:- Simulation Processing Flow

Scenario setup involves creating the roadway, adding scenario actors, and defining sensor and sensor attachment to actors. For each time step, sensor detections are generated, along with any false alarms. These detections and false alarms are fed to the tracking algorithm, which creates, maintains, and prunes tracks. Actors are then moved to their next positions, and interference levels are adjusted based on changed interactions between the ego vehicle and other radar systems in the scene. Finally, plots and metrics measuring performance of the ego vehicle sensor are produced.

To implement our simulations, we chose to use the MATLAB platform (from MathWorks), with the add-on ADAS toobox.[1] Introduced in 2017, the ADAS toolbox provided most of the capability we needed. In those instances where it did not provide the desired interface, it proved easy to extend.

5.3.1 **Scenario generation**

The ADAS toolbox provides methods for defining roadways, actors (vehicles and pedestrians), and motion profiles for those actors. The roadways are constructed from two-lane road segments, defined by a set of center-points (x, y, z) along the segment. The center-points are connected by piecewise clothoid curves. The segments can be banked, and the ends of the segment can be connected to form a loop. Multiple segments can be added to a scenario to produce intersections, etc., as shown in Figure 10. Very limited consistency checking is done by the software, so the scenario designer must insure that the result matches real world scenarios, e.g. roads intersecting with non-matching banking.

[1] MathWorks (2017). Define Road Layouts. *MathWorks.* The MathWorks, Inc., Natick, MA. www.mathworks.com/help/driving/examples/define-road-layouts.html

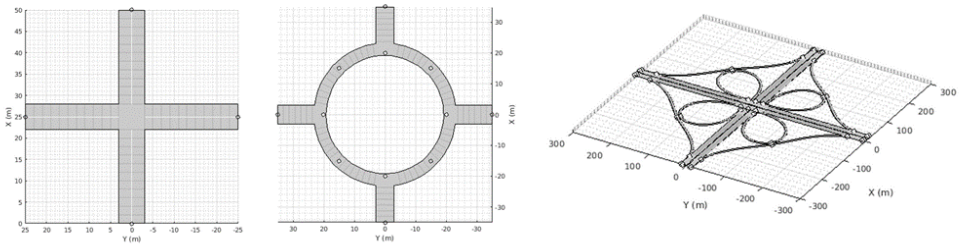

Figure 10:- Examples of ADAS generated roadways[2]

Vehicles are added to the roadway by specifying a set of waypoints and velocities. The waypoints, like the road centers, are x, y, z coordinates. In the software as delivered by MathWorks, there is no way to control the assignment of colors to the vehicles; we accomplished custom color assignments by creating and a local copy of the code file containing the color assignments (lines.m), and modifying it with our desired colors. An example of displays with custom color assignments are shown in Figure 11. In this case, the ego vehicle is blue, the target vehicle is red, and all the interferers are yellow.

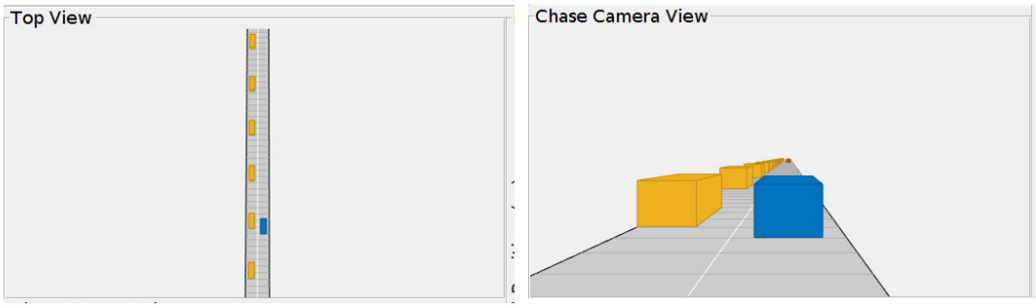

Figure 11: Generated roadway with vehicles that contain custom color assignments

5.3.2 **Sensor definition and placement**

To measure the dynamic environment, sensors can be attached to the vehicles. The goals of our simulations were to measure radar detections and performance, but the ADAS software can also simulate vision systems.

Sensors are attached to vehicles. Once a sensor is attached, it moves with the vehicle as it traverses the roadway. Each sensor has an update rate, which controls the number of detections the sensor generates, and may be different than the update rate of the scenario (i.e., movement of the vehicles).

The values of these parameters used in our simulations are shown in Table 5. Table 6 provides a description of radar parameters. The MATLAB ADAS toolbox object properties of each radar, and the associated tracker, are shown in *Appendix: Matlab ADAS Toolbox, Radar and Tracker Objects*.

[2] Ibid.

An example display of an ego vehicle radar azimuth field of view is shown in Figure 12.

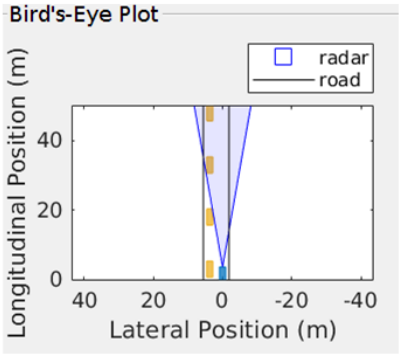

Figure 12: Overhead view showing radar beam indicating azimuth field of view.

5.3.3 **Sensor detection modeling**

Detectability of targets is governed by three inter-related parameters: Probability of false alarm (PFA), probability of detection (PD), and signal-to-noise ratio (SNR). Probability of false alarm relates to the number of false detections that are allowed to occur. To ensure that detections of real targets are generated, some amount of false alarms must be allowed. For our simulations, the PFA was set to 1e-6, meaning that a false alarm will occur every 1,000,000 detections. This PFA was selected to be on the low end of PFA values that are valid for Albersheim's equation (1e-7 < PFA < 1e-3), based on industry practices of limiting false alarms. The expectation is that some false alarms will be eliminated via the tracking system, since unlike detections from real vehicles, the false alarms are not related in a physically meaningful way.

Once an acceptable level of false alarms has been set, the relationship between the PD and SNR is defined via a receiver operating characteristic (ROC) curve, an example of which is shown in Figure 13. This ROC curve is derived from well understood radar reflection phenomenology. In the ADAS toolbox, radar reflections are assumed to be from non-fluctuating targets, with non-coherent pulse integration, generated via Albersheim's detection equation (Richards, 2005). While this model for reflections is adequate for many uses, with more time and effort, this equation could be replaced with a richer model from Snidman's equations (Richards, 2005), based on Swerling models that provide for fluctuating responses generated from collections of potentially non-homogeneous scattering mechanisms of targets.

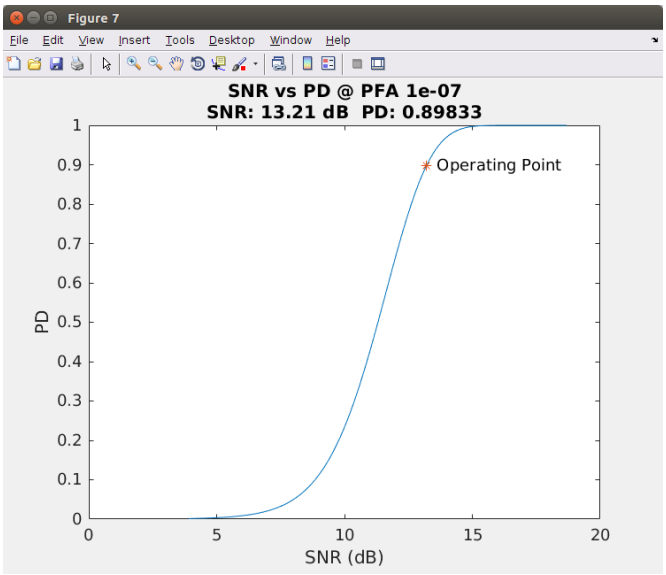

Figure 13: Example ROC curve relating SNR and PD given desired PFA

Detections are generated on a per-time-step basis. First, actors within the scenario are moved to their current position. Next, point targets are generated for the scene. The region-of-interest (ROI) is defined by the orientation and field-of-view of the radar. This ROI is sub-divided based on the minimum spacing defined by the azimuth and range resolutions as demonstrated in Figure 14, (in these simulations, elevation resolution is infinity, i.e., responses cannot be separated by height). Actors are represented as 6-sided cuboids. At most three sides of an actor are visible to the radar at any time. Point targets are generated wherever the side of an actor occupies one of the sub-divisions of the ROI.

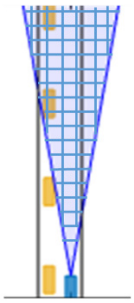

Figure 14: Example of subdividing radar beam to identify point target responses

Each point target is assigned a radar cross section (RCS) value. This is the idealized response of the target at the given angle, without accounting for distance between the sensor and the target. Each actor is assigned a set of RCS values, which can differ with illumination angle. These set of RCS values are interpolated to get the point target response given the per-time-step illumination angle of the target. For our simulations, all vehicles are assigned an RCS value of 10 dBsm for all angles, which has been found in previous work (Buller & LeBlanc, 2012) to be a good estimate of vehicle cross-section.

Point targets are then eliminated based on range rate. Range rate is a measure of the radar's ability to discern changes in relative range between the ego and target vehicles. The limit on this ability comes from the rate at which the radar can transmit pulses, driven by an engineering tradeoff between expected maximum vehicle velocities, maximum range extent, and cost of the radar system. Point targets outside the minimum/maximum range rate are considered spurious and ignored.

Since the RCS of the target does not account for the distance between the sensor and point target, this number must be converted into the SNR at the point target. The SNR for each point target is derived using the following equation:

$$SNR_T = SNR_R - RCS_R + 40log10(Rng_R) - 40log10(Rng_T) + RCS_T$$

where SNR_T is the calculated SNR of the point target (in dB), SNR_R is the reference SNR (in dB) derived from the SNR versus PD ROC curve, RCS_R is the reference RCS (in dBsm), Rng_R is the reference range (in meters), Rng_T is the range to the point target (in meters), and RCS_T is the target RCS (in dBsm) at the location of the point target.

Once the SNR at the point target is known, a noise model is applied to the point target positions, to simulate uncertainty in location measurement accuracy. This noise model is driven by the SNR at the point target, with separate models for azimuth, elevation, range, and range rate. Each of the models is based on a zero mean normal distribution, with user settable standard deviation:

$$est = truth + \frac{1}{\sqrt{2\pi\sigma^2}} e^{-\frac{x^2}{2\sigma^2}}$$

where $truth$ is the azimuth, elevation, range, or range-rate derived from the ground truth, σ is the user defined per-estimate standard deviation, x is a uniform random number, and est is the resulting perturbed estimate.

Point targets that occupy the same resolution cell are then merged, since the radar would be unable to distinguish between the separate points. The SNR in the resolution cell becomes the sum of the merged point targets, with the response position information coming from the point target with the highest SNR.

Those resolution cells that contain a non-zero response are then examined to determine if a detection should be generated. To decide if a detection is to be generated, the PD versus SNR ROC curve is indexed using the SNR at the resolution cell to determine the probability that a detection will be generated. A uniformly distributed random number is generated, and a detection is generated if the random number is below the PD. If a detection is generated, error statistics for the azimuth, range, and range-rate estimates are also computed.

The total number of false alarms generated are chosen by calculating the total number of resolution cells for one sweep of the radar and multiplying that number by the false alarm rate. If false alarms are generated, the range and azimuth locations of the false alarms are chosen at random from a uniform distribution. False alarms are assumed to be marginal detections, therefore the SNR of each false alarm is set by applying Albersheim's equation (Richards, 2005) at the detection threshold level. Finally, the false alarms are grouped together with the target detections into one set of radar detections.

The radar detections are then fed into a tracking algorithm in order to attempt to group the current detections with previous detections and tracks. Any current detections that cannot be assigned to previous tracks are used to create new tracks. Previous tracks that are assigned new detections are updated and confirmed. Any tracks that did not get a new detection are initially coasted and, if they continue to fail to obtain detections in the future, are eventually deleted. The default tracker used in the ADAS toolbox, and also our study, is a constant velocity linear Kalman filter.

The main metric used in determining the ability of the radar to detect a target in the presence of interference and noise is the terminal track range. This is the maximum range of a continuous track of the target. In other words, this is how far out the radar was able to initially detect the target and maintain that track through the completion of the simulation.

6 Scenarios

This section lists the scenarios that were selected for simulation. The selection is based on scenarios that apply to common traffic situations, with a focus on those that were identified as concerning in the literature, and during our interviews with industry. The scenarios consider interference due to direct illumination (radar antennas facing each other), as well as, reflected interference (radars illuminating the same target).

The simulation scenarios are designed to spotlight typical situations where interference can be expected, and investigate the effects of interference from other vehicles on the ability of the ego vehicle to maintain a track on the target vehicle.

A summary of the scenarios is shown below in Figure 15.

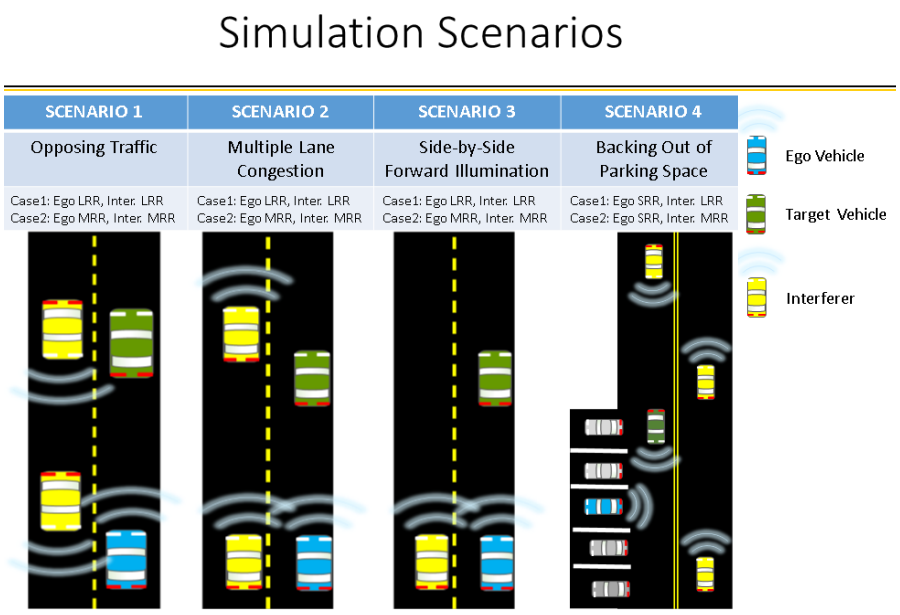

Figure 15: Summary of the Scenarios tested in simulation. The impacts are estimated for the performance of the Ego Vehicle (blue) to track a Target Vehicle (green) in the presence of Interferers (yellow).

An additional pair of results, Scenario 5, has been generated to compute the expected interference level for radars facing each other in traffic, although these have not been implemented in the full simulation. The situation, shown in Figure 16, is important because the geometry of the pair is the worst-case scenario.

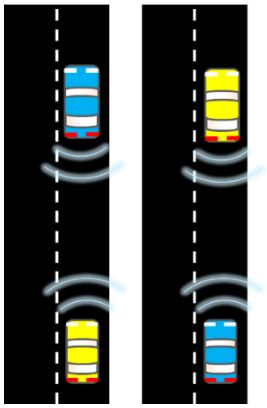

Figure 16: At left, the ego vehicle in blue, operates a rear looking radar and faces interference from the forward-looking radar of the yellow car. At right, the roles are reversed.

6.1 Scenario result format

Each scenario result contains a scenario depiction, a table and a number of plots. The depiction shows the concept behind the scenario, and a display showing the position of the vehicles at the end of the scenario. This is followed by a table that lists the power levels of the target, P_T, clutter, P_C, and interferer, P_I, at the reference range R_0 documented in Table 5. The table is followed by a set of plots displaying power levels of P_T, P_C, and P_I versus range for each radar type in the scenario, and for both the 76-77 GHz and 76-81 GHz bands.

In the case of the reference target and the clutter, the power received is localized to a range bin. The power at the target P_T at range R is calculated as

$$P_T(R) = \frac{P_{tx} G_{tx} G_{rx} \lambda^2 \sigma_T}{(4\pi)^3 R^4}$$

where P_{tx} is the transmitted power, G_{tx} is the gain of the transmit antenna, G_{rx} is the gain of the receive antenna, λ is the wavelength (derived from transmitter center frequency f_c via $\frac{c}{f_c}$ where c is the speed of light), σ_T is the radar cross-section of the target, and R is the range to the target. σ_T is 10 dBsm for these scenarios. All values are linear scale (not dB) when used in this equation.

An automotive radar is always operating in a clutter filled environment. For the purpose of these scenarios, the clutter is modeled as smooth asphalt. To compute the power returned from the clutter, the clutter radar cross-section σ_C is estimated by determining the area of a range-bin intercepting the road at range R, then multiplying by the clutter coefficient σ_0 at the incidence angle of the radar.

$$\sigma_C = \rho_a \rho_r \sigma_0$$

σ_0 is set to -30 dB, which approximates the return from asphalt for a radar with an 88° incidence angle (Sarabandi, Li, & Nashashibi, 1997).

Once the radar cross-section for the clutter is defined, then the equation for the power of the clutter P_c at range R is:

$$P_c(R) = \frac{P_{tx} G_{tx} G_{rx} \lambda^2 \sigma_C}{(4\pi)^3 R^4}$$

The mean power from the interference is treated as non-coherent, Gaussian white noise. For scenarios 1, 2, and 4, this assumption is used for estimating average interference levels. The mean interference power is, therefore, distributed uniformly over the range bins. This means that the interference at a given range is less than the total mean interference power by the compression gain in the radar model reported in Table 5. Additionally, the mean interference power can be further reduced by increasing the band available to the radar, due to a decrease in spectral collision, i.e., the interference is estimated under the assumption that the center frequency of each radar is selected at random, uniformly distributed, across the available band. Thus, the results show that the interferer suffers a 7 dB reduction in the case where the allowable band is increased by a factor of 5 (i.e., using 76-81 GHz, rather than 76-77 GHz).

Scenarios 1 and 4 are examples of the interference being received directly from the interferer radar (i.e., direct path instead of reflected). The equation for the mean interference power in scenarios 1 and 4 is calculated as

$$P_{I1} = \frac{I_1}{\mu_{spacing} * RangeBinCount * BandFactor}$$

where I_1 is the statistical interference calculated in 5.2.1, $\mu_{spacing}$ is the mean spacing distance between interferer vehicles, $RangeBinCount$ is the number of range bins in the compressed radar pulse (i.e., the effect of the compression gain), and $BandFactor$ is factor for comparing different widths of the available spectral band, 1 for 76-77 GHz, and 5 for 76-81 GHz. Note that the range to the target does not play a role here since the interferer transmissions are reaching the ego radar receiver directly without reflecting off the target.

Scenario 2 is similar to 1 and 4 in that the interferer level is calculated stochastically, but the energy from the interferer arrives at the ego receiver after reflecting off the target. This requires inclusion of the distance between the ego vehicle and target in the calculation:

$$P_{I2}(R) = \frac{I_2}{R * \mu_{spacing} * RangeBinCount * BandFactor}$$

where $I2$ is the stochastic interference calculated in 5.2.2, and R is the distance between the ego and target vehicles.

Scenario 3 is unique in that it contains only one interferer vehicle, so the interferer calculation does not contain a stochastic component. The interferer level for this scenario is based simply on the bi-static radar equation

$$P_{I3}(R_{tx}, R_{rx}) = \frac{P_{tx} G_{tx} G_{rx} \lambda^2 \sigma_T}{(4\pi)^3 R_{tx}^2 R_{rx}^2}$$

where R_{tx} is the range from the transmitter (interferer) to the target, and R_{rx} is the range from the receiver (ego) to the target.

Given the calculation of the interferer power, the signal-to-interferer/noise at the target ($SINR_T$) can then be calculated:

$$SINR_T = SNR_T + \underbrace{N_{dB} - 10\log_{10}(P_I + N)}_{\text{Adjustment for interferer}} + \underbrace{10\log_{10}(P_{tx})}_{\text{Adjustment for RADAR power level}}$$

with SNR_T is as described in 5.3.3, P_I is P_{I1}, P_{I2}, or P_{I3} based on the intended scenario, and the noise estimate is:

$$N = kTB_{Rx}f_n$$

with k: $Boltzmann's\ const.$ $\left(1.38\,x10^{-23}\ \frac{W}{Hz \cdot K}\right)$, T: $system\ temperature$ $(290K)$, B_{Rx}: $Receiver\ Bandwidth$ (Hz), and f_n: $Noise\ factor$ $(unitless)$.

Following the power comparisons are three plots showing the output of the tracker. The first track plot displays those tracks that were generated in a noise free environment. The second and third plots show tracks formed in interference conditions, both at the 76-77 GHz band, and 76-81 GHz band.

In each track plot, only those tracks that both contained at least one detection on the target vehicle, and continued until the end of the simulation, are shown. For each detection within a track, a marker is displayed at the estimated position of the detection, and an error ellipse is drawn around the detection to demonstrate the confidence level of the tracker. As the distance between the ego and target vehicle decreases, the signal-to-noise level increases, causing these error ellipses shrink.

6.2 Scenario 1 - Interference from opposing traffic

Scenario 1 considers the ego vehicle with a forward-looking radar gaining on a target vehicle, while vehicles approaching the ego vehicle in the opposing lane contain radars transmitting in the direction of the ego vehicle as summarized in Figure 17 and Figure 18. In this scenario the interferer levels are determined statistically based on mean separation of vehicles, which is 15 meters. The interferer level is held constant due to the steady stream of direct path interference.

- Scenario duration is 12 s
  - Time from start until Ego will collide with Target
- Vehicles
  - Ego vehicle (blue), 80 kph
  - Target vehicle (green), 20 kph, ahead of ego
  - Interfering vehicles (yellow), 80 kph
    - **Traveling in left lane, opposite direction to ego**
      - Direct-path interference
    - Continuous stream, uniform vehicle spacing between 10 to 20 m
    - Interference levels constant, represented by stochastic interference
  - US lane spacing is nominally 3.7 m
- Radars
  - Forward LRR and MRR

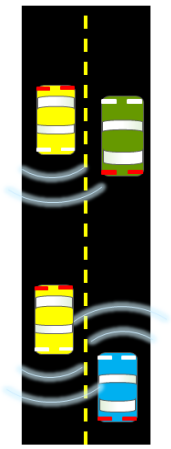

Figure 17: Scenario 1 Depiction

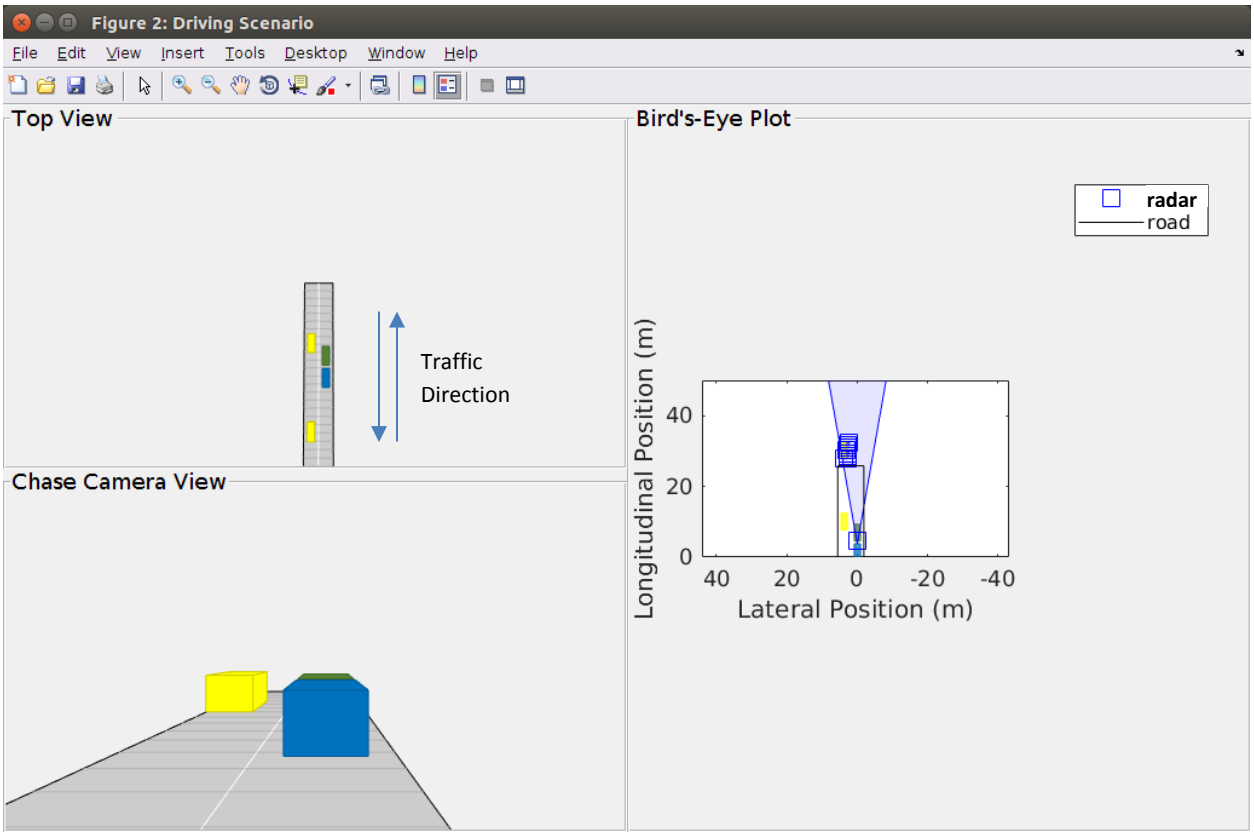

Figure 18: Position of vehicles at end of Scenario 1

The power levels for scenario 1 are tabulated in Table 8. In all cases, the power received from the interference caused by the oncoming traffic has a mean value significantly above the reference target at the reference range found in Table 5.

Table 8: Received power from reference target, clutter, and interference power in reference range bin, P_T, P_C, and P_I, respectively, for Scenario 1: Interference from opposing traffic.

dB Watts	Ego Radar	Other Radar	P_T	P_C	P_I
76-77 GHz	LRR	LRR	-107	-128	-73
	MRR	MRR	-115	-138	-81
76-81 GHz	LRR	LRR	-107	-129	-80
	MRR	MRR	-115	-138	-88

The plots in Figure 19 show that the target power levels remain below the interferer levels until the target becomes closer than 25 meters.

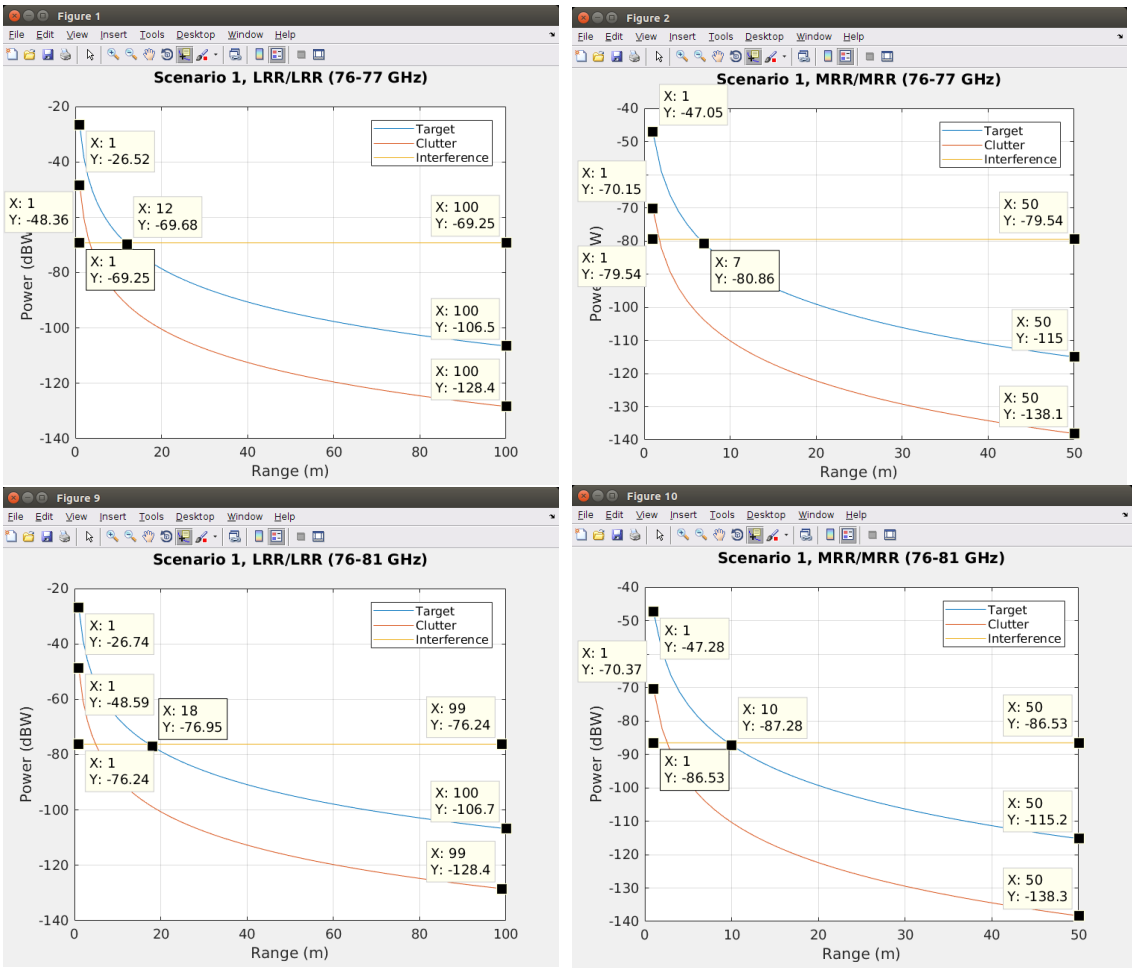

Figure 19: Comparison of target, clutter, and interferer power with various radars at various ranges

For the ego radar to perform near specification, the radar must mitigate many decibels of power from interference. To achieve this, the radar must employ mitigation techniques and avoid receiver saturation. The techniques that have been suggested in interviews with industry, and reported in the literature, which apply here include: polarization specification, digital beamforming, and detect and repair time domain signals. Depending on the environment and implementation of these techniques, the available mitigation may be on the order of 40 dB. This would involve harmonization of the antenna's polarizations. Additional mitigation may be available with further techniques: sniff-and-avoid, narrow band processing, and waveform coding.

The interference power is used as a surrogate for the noise power in simulation with Matlab's ADAS toolbox.

6.2.1 **Scenario 1, Long-range radar system impacts**

This version of scenario 1 examines the situation where all vehicles have long-range radars. While the no-interference plot shows good detection and tracking at almost 200 meters, (Figure 20), this degrades significantly when interference is added, (Figure 21). Some of this loss of detection can be recovered by using the wider 76-81 GHz band, which permits a higher success of spectral avoidance, (Figure 22).

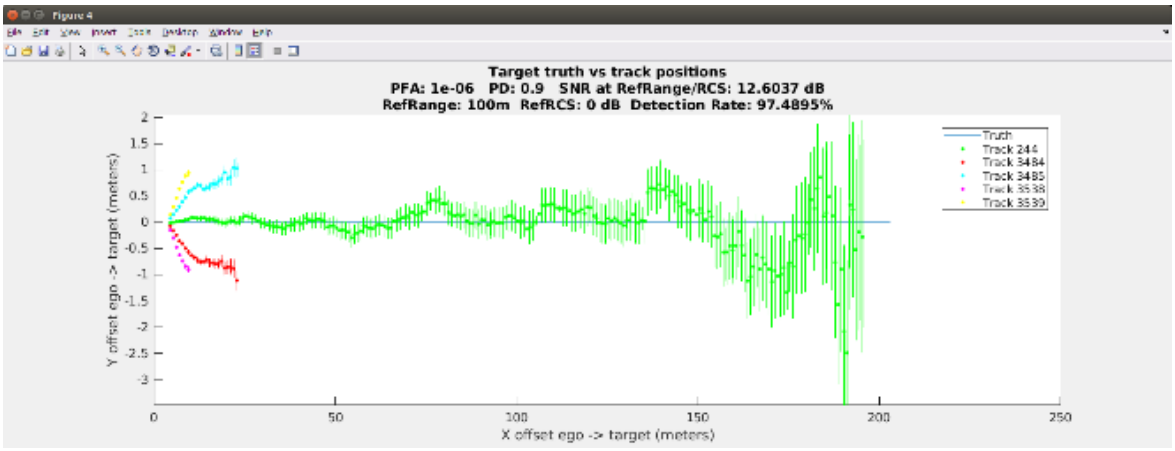

Figure 20: Plot of persistent target tracks from Scenario 1, long-range radar with no interference

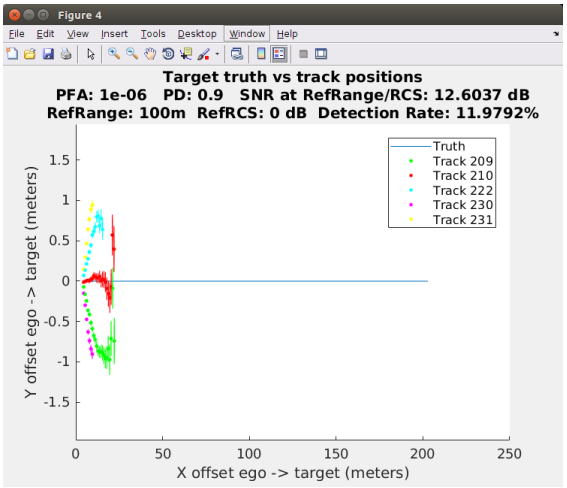

Figure 21: Plot of persistent target tracks from Scenario 1, long-range radar, with interference, for the case of 76-77 GHz band

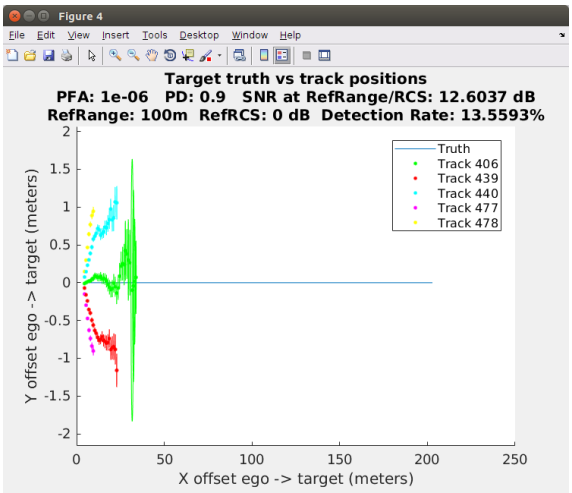

Figure 22: Plot of persistent target tracks from Scenario 1, long-range radar, with interference, for the case of 76-81 GHz band

6.2.2 **Scenario 1, Mid-range radar system impacts**

This version of scenario 1 examines the situation where all vehicles have mid-range radars. Due to the reduction in transmit power, the detection distance is greatly reduced compared to the long-range radar, but in the interference-free case tracks are maintained out to almost 50 meters

(Figure 23). This is drastically reduced with the addition of interference (Figure 24), and again, using the wider band recovers some detection distance, (Figure 25).

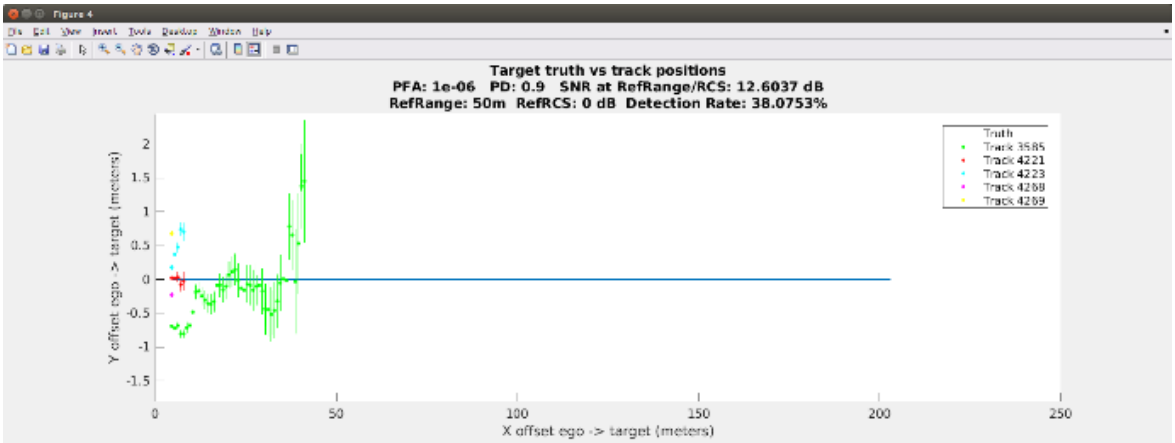

Figure 23:- Plot of persistent target tracks from Scenario 1, mid-range radar with no interference

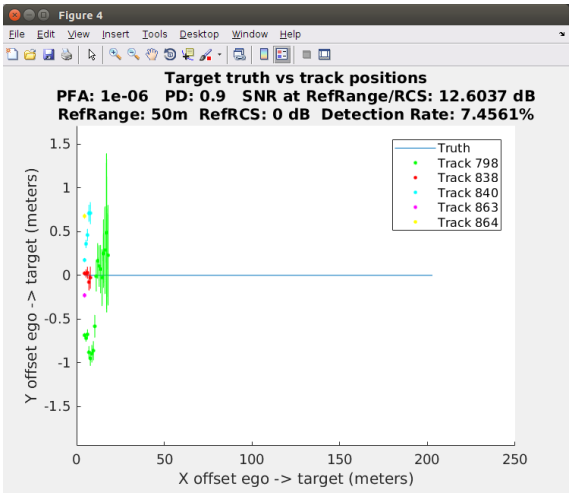

Figure 24: Plot of persistent target tracks from Scenario 1, mid-range radar, with interference, for the case of 76-77 GHz band

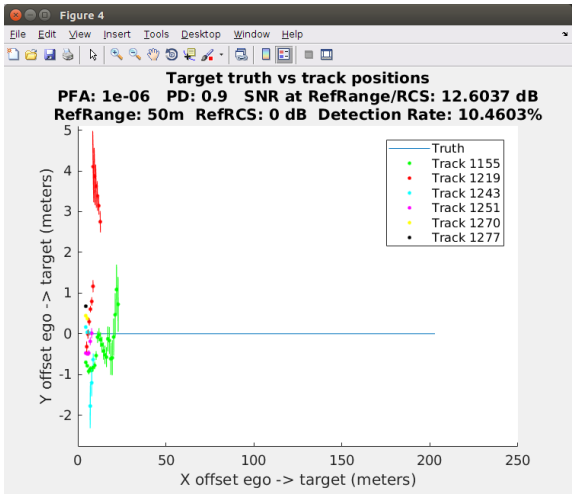

Figure 25: Plot of persistent target tracks from Scenario 1, mid-range radar, with interference, for the case of 76-81 GHz band

6.3 Scenario 2 - Interference from passing traffic

Scenario 2 considers the ego vehicle with forward-looking radar gaining on a target vehicle, while traffic in the next lane is passing at a higher speed as shown in Figure 26 and Figure 27. The passing vehicles have radars that also illuminate the vehicle ahead. In this scenario the interference comes from reflected energy off the ego vehicle, and interference levels are determined statistically based on mean separation of vehicles, which is 15 meters. The levels change over time as the ego vehicle approaches the target vehicle due to the reduced reflection distance.

- Scenario duration is 24 seconds
  - Time from start until Ego will collide with Target, Interferer passes Target
- Vehicles
  - Ego vehicle (blue), 100 kph
  - Target vehicle (green), 70 kph, ahead of ego
  - Interfering vehicles (yellow), 120 kph
    - **Traveling in left lane, same direction as ego**
      - Reflected path interference
    - Continuous stream, uniform vehicle spacing between 10 to 20 m
    - Interference levels change with distance between ego and target, represented by stochastic interference
  - US lane spacing is nominally 3.7 m
- Radars
  - Forward LRR and MRR

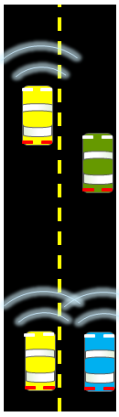

Difference from Scenario 1
- Interferers same direction as ego
  - Interference from reflection off target
- Uses range from ego to target to calculate interferer level

Figure 26: Scenario 2 Depiction

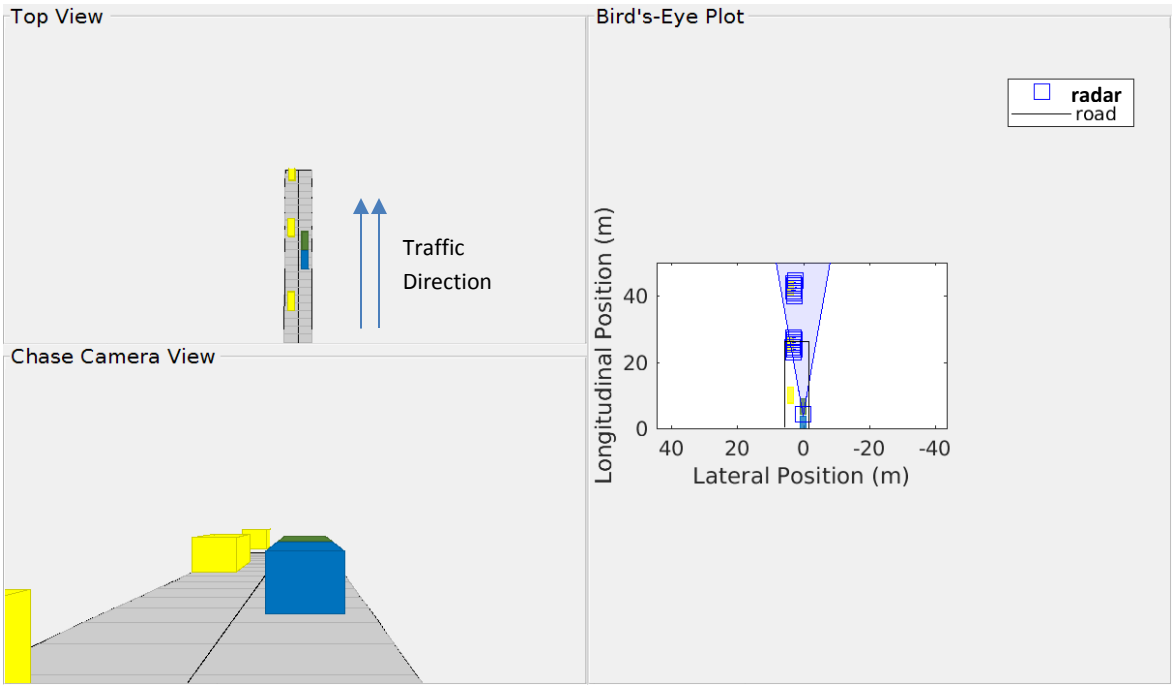

Figure 27: Position of vehicles at end of Scenario 2

The power levels for scenario 2 are tabulated in Table 9. The mean level of the power received from the interference caused by the passing traffic is always below the level of the reference target at the reference range found in Table 5, and in fact is always lower in all ranges up to the reference range, as seen in the accompanying power level plots in Figure 28. It is interesting to note that in the case of the MRR with band 76-77 GHz, the separation between the target and the interferer is only 2 dB Watts at the reference range.

Table 9: Received power from reference target, clutter, and interference power in reference range bin, P_T, P_C, and P_I, respectively, for Scenario 2: Interference from passing traffic.

dB Watts	Ego Radar	Other Radar	P_T	P_C	P_I
76-77 GHz	LRR	LRR	-107	-128	-110
	MRR	MRR	-115	-138	-115
76-81 GHz	LRR	LRR	-107	-129	-117
	MRR	MRR	-115	-138	-122

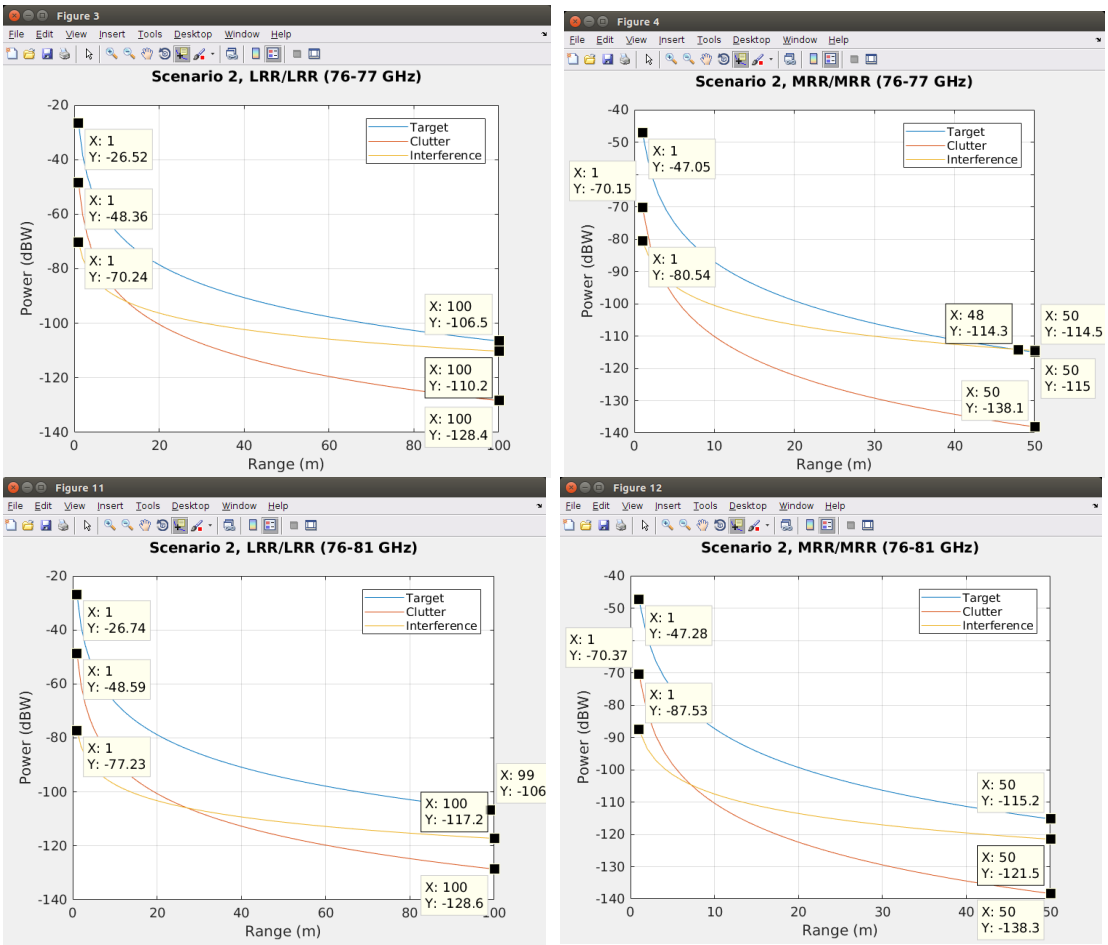

Figure 28: Comparison of target, clutter, and interferer power with various radars at various ranges

6.3.1 **Scenario 2 – Long-range radar system impacts**

This version of scenario 2 examines the situation where all vehicles have long-range radars. The plots in Figure 29, Figure 30, and Figure 31 show that the interference has no effect on the ego radar's ability to track the target, i.e., the resulting tracks where interferers are present are the same as when there is no interference.

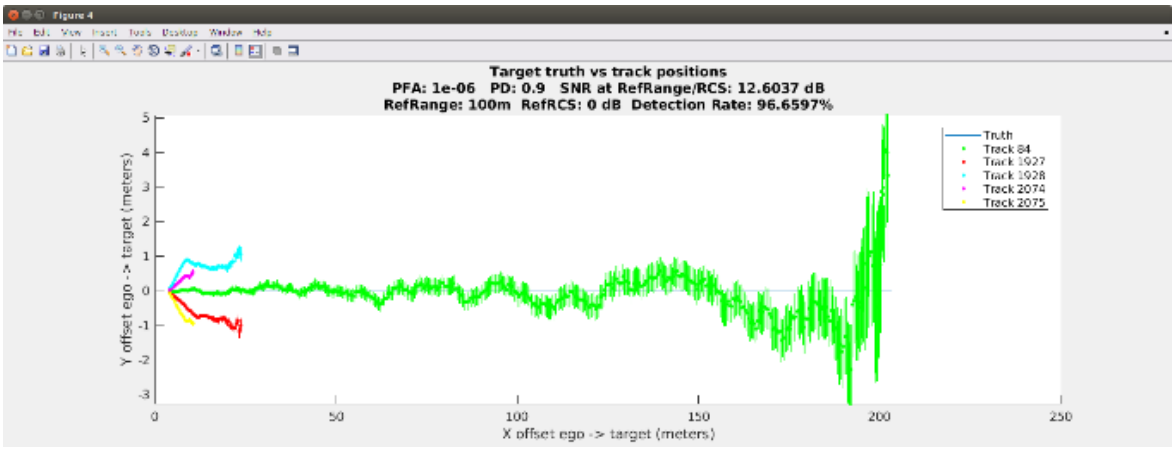

Figure 29: Plot of persistent target tracks from Scenario 2, long-range radar with no interference

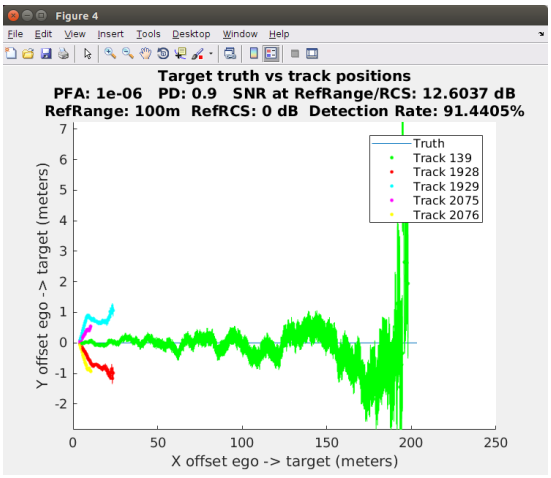

Figure 30: Plot of persistent target tracks from Scenario 2, long-range radar, with interference, for the case of 76-77 GHz band

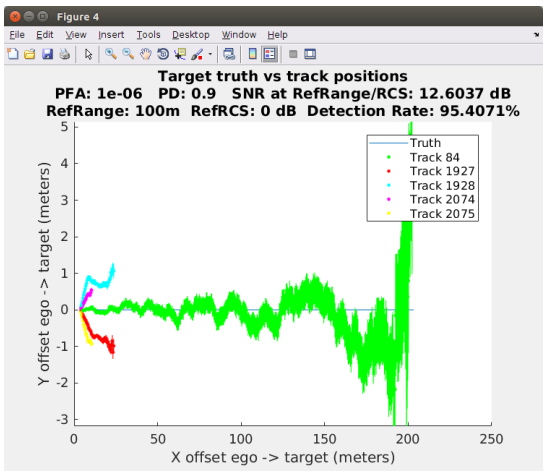

Figure 31: Plot of persistent target tracks from Scenario 2, long-range radar, with interference, for the case of 76-81 GHz band

6.3.2 Scenario 2 – Mid-range radar system impacts

This version of scenario 2 examines the situation where all vehicles have mid-range radars. As in the mid-range radar case, the plots in Figure 32, Figure 33, and Figure 34 show that the interference has no effect on the ego radar's ability to track the target.

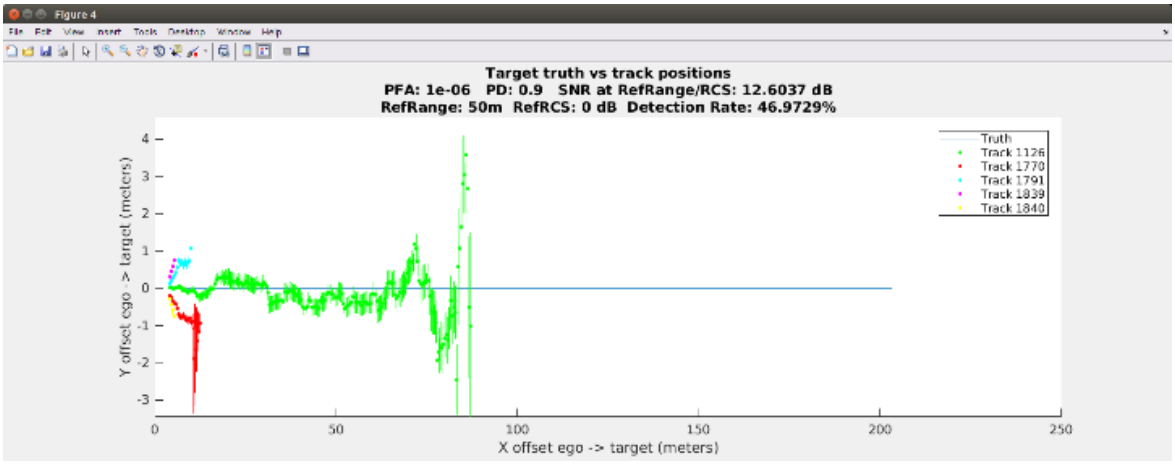

Figure 32: Plot of persistent target tracks from Scenario 2, mid-range radar with no interference

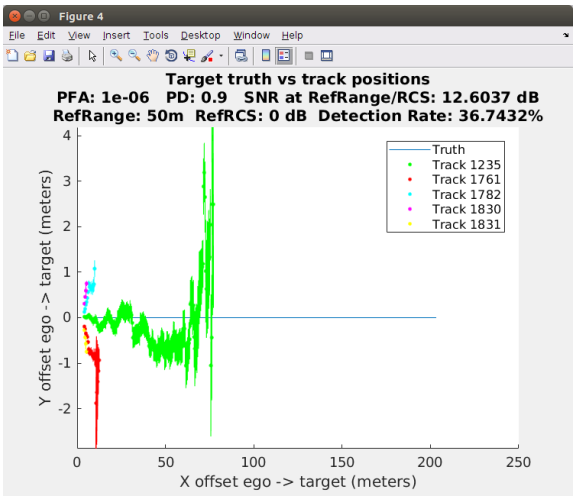

Figure 33: Plot of persistent target tracks from Scenario 2, mid-range radar, with interference, for the case of 76-77 GHz band

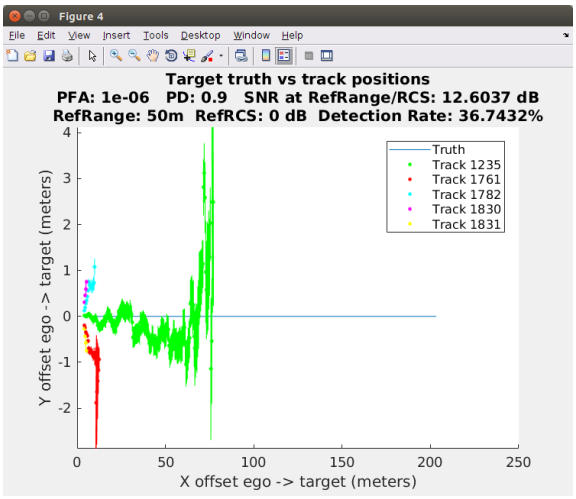

Figure 34: Plot of persistent target tracks from Scenario 2, mid-range radar, with interference, for the case of 76-81 GHz band

6.4 Scenario 3 – Side-by-side forward illumination

Scenario 3 considers the ego vehicle with a forward-looking radar gaining on a target vehicle, while a single vehicle in the next lane is passing at a higher speed as summarized in Figure 35. The passing vehicle has a radar that also illuminates the vehicle ahead. In this scenario the interference comes from reflected energy off the ego vehicle, and interference levels are derived from the bi-static radar equation, changing over time as a function of the changing path the

interference follows from the interferer vehicle, to the target vehicle, then to the ego vehicle's receiver.

- Scenario duration is 24 seconds
  - Time from start until Ego will collide with Target, Interferer passes Target
- Vehicles
  - Ego vehicle (blue), 100 kph
  - Target vehicle (green), 70 kph, ahead of ego
  - One interfering vehicle (yellow), 120 kph
    - **Traveling in left lane, same direction as ego**
      - Reflected interference
    - Interference levels change with distance between (interferer and target + ego and target), using radar equation
  - US lane spacing is nominally 3.7 m
- Radars
  - Forward LRR and MRR

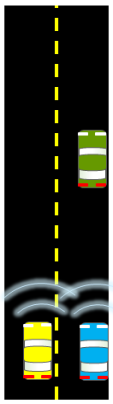

Differences from Scenario 2

- One interferer
- Uses range from interferer to target **and** ego to target
- Uses radar equation to calculate interferer level (not stochastic)

Figure 35: Scenario 3 Description

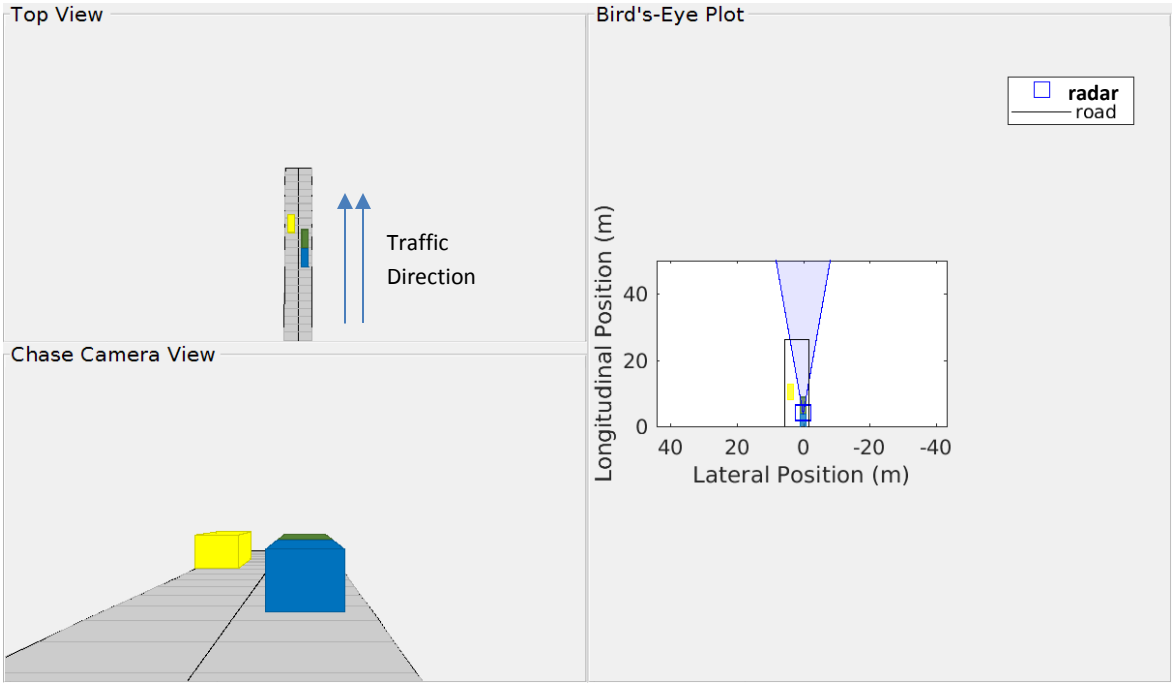

Figure 36: Position of vehicles at end of Scenario 3

The power levels for scenario 3 are tabulated in Table 10. The table shows that the power level of the interferer is higher than for the target in all cases except the wider band 76-81 GHz case, but is much less significant than in scenario 1 with the direct path interference. Looking at the plots in Figure 37, it is clear that the difference between interferer and target is relative small, and that a wider band makes a significant difference in the amount of distance at which the target level rises above the interference level.

Table 10: Received power from reference target, clutter, and interference power in reference range bin, P_T, P_C, and P_I, respectively, for Scenario 3: Side-by-side forward illumination

dB Watts	Ego Radar	Other Radar	P_T	P_C	P_I
76-77 GHz	LRR	LRR	-107	-128	-96
	MRR	MRR	-115	-138	-110
76-81 GHz	LRR	LRR	-107	-129	-103
	MRR	MRR	-115	-138	-117

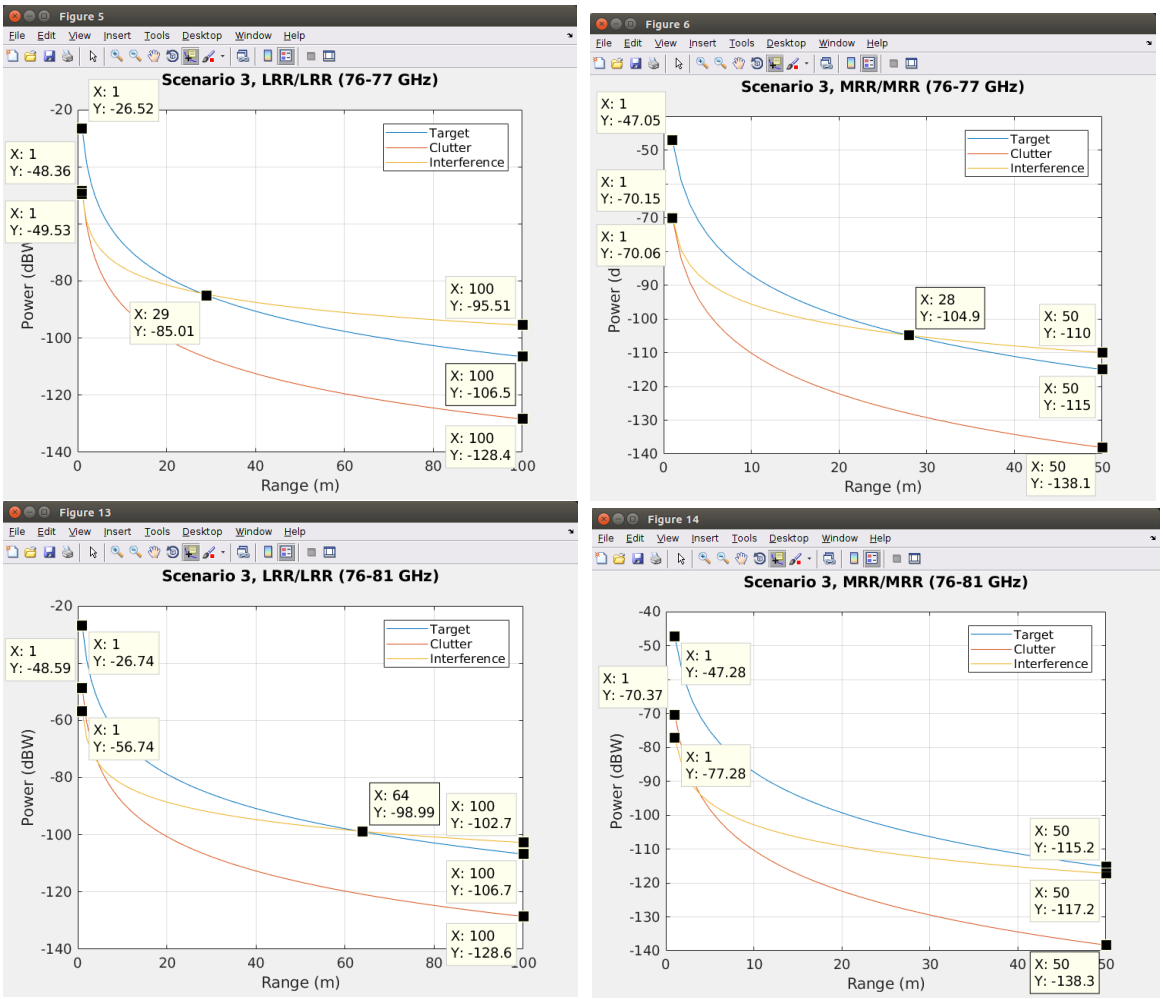

Figure 37: Comparison of target, clutter, and interferer power with various radars at various ranges

6.4.1 **Scenario 3 – Long-range radar system impacts**

This version of scenario 3 examines the situation where the ego and interferer vehicle both have long-range radars. The plots show that the interference has no significant effect on the ego's ability to track the target, i.e., the cases where interferers are present (Figure 39 and Figure 40) are similar to when there is no interference (Figure 38). This is due to the mitigation of the interference due to compression gain within the ego vehicle's radar system.

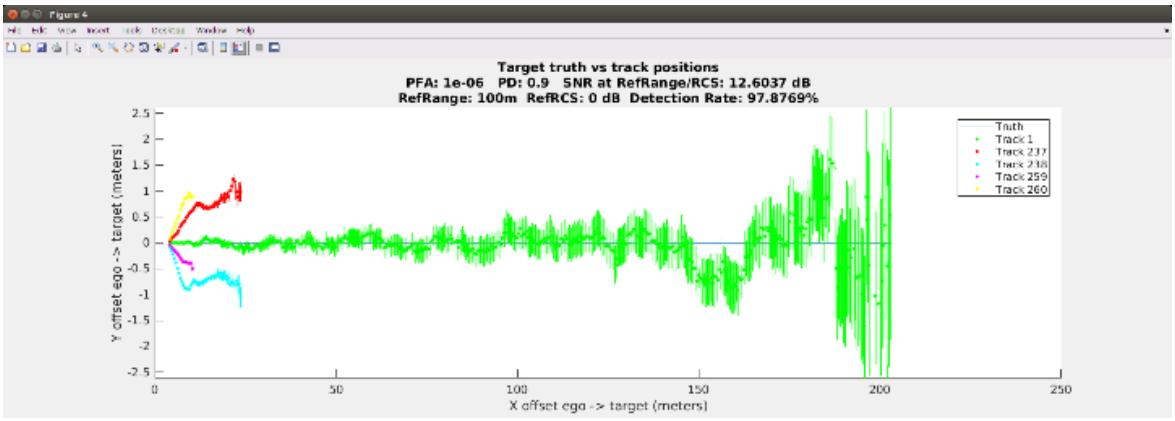

Figure 38: Plot of persistent target tracks from Scenario 3, long-range radar with no interference

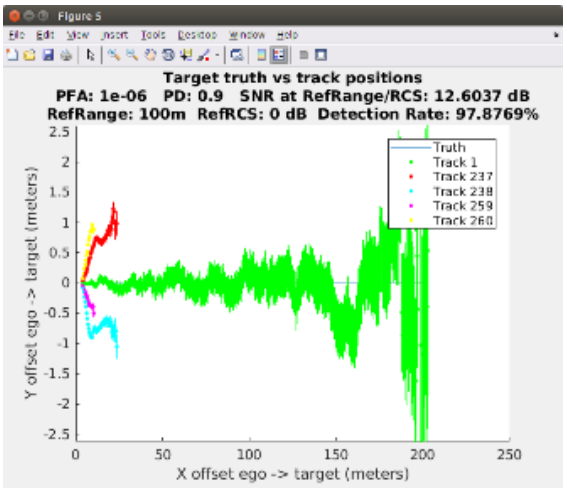

Figure 39: Plot of persistent target tracks from Scenario 3, long-range radar, with interference, for the case of 76-77 GHz band

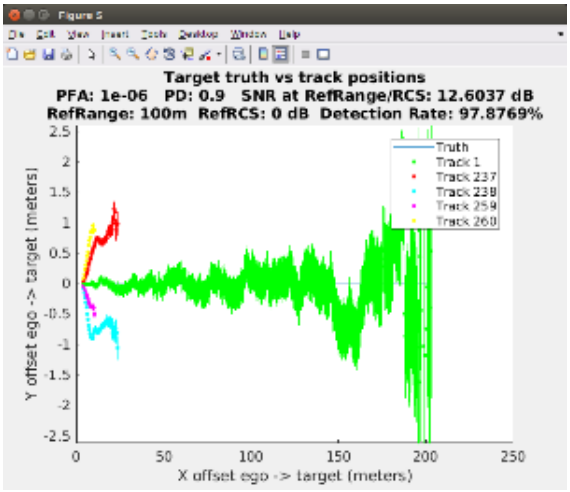

Figure 40: Plot of persistent target tracks from Scenario 3, long-range radar, with interference, for the case of 76-81 GHz band

6.4.2 **Scenario 3 – Mid-range radar system impacts**

This version of scenario 3 examines the situation where the ego and interferer vehicle both have mid-range radars. Unlike the long-range radar case, compared to the no-interference case in Figure 41, the plots in Figure 42 and Figure 43 show that the interference reduces the distance at which the ego can track the target vehicle. Using a wider band does not help in this situation.

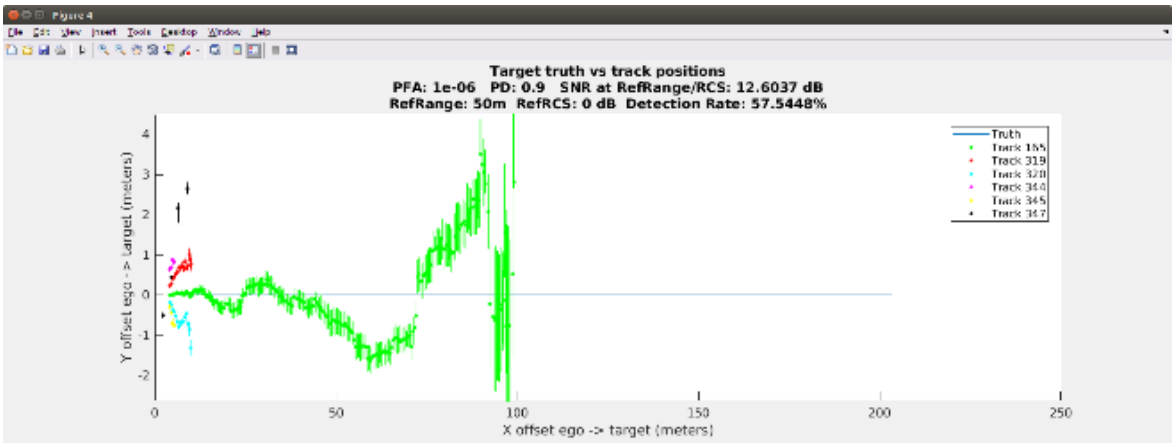

Figure 41: Plot of persistent target tracks from Scenario 3, mid-range radar with no interference

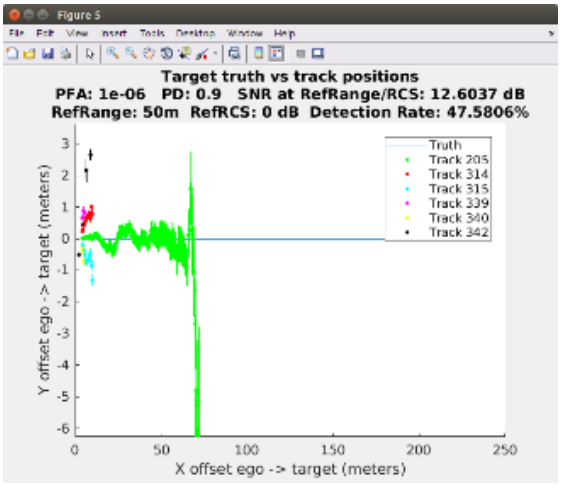

Figure 42: Plot of persistent target tracks from Scenario 3, mid-range radar, with interference, for the case of 76-77 GHz band

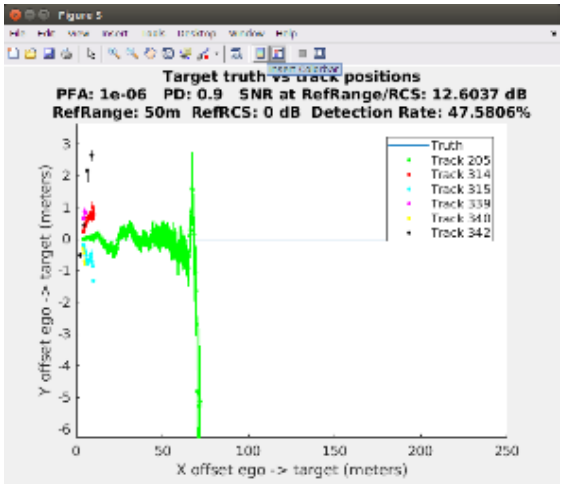

Figure 43: Plot of persistent target tracks from Scenario 3, mid-range radar, with interference, for the case of 76-81 GHz band

6.5 Scenario 4 – Backing out of a parking space

Scenario 4 simulates backing out of a parking spot into a busy road as shown in Figure 44 and Figure 45. This illustrates the interaction between the ego vehicle's rear-looking short-range and the interferer's longer-range radars. For this scenario, the signals received by the ego are coming from the side-lobes of the LRR interferer's radar beam, and a mixture of main-lobe and side-lobe illumination from the MRR interferer's radar beam. The side-lobe illumination has a reduction in the antenna gain, resulting in a lower interference level than would be experienced from the main-beam (as in scenario 1).

- Scenario duration is 3.6 seconds
  - Time from start until Target passes Ego
- Vehicles
  - Ego vehicle (blue) backing out, stationary
  - Target vehicle (green), 40 kph
    - Radiating, so contributes to stochastic interference
    - Begins at 40 meters down range
  - Interfering vehicles (yellow), 40 kph
    - **Moving both directions**
    - Interference levels constant, received in side-lobes only
- Radars
  - Ego has SRR, interferers are forward LRR and MRR

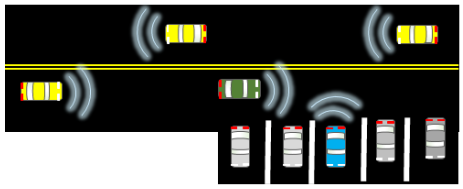

Figure 44: Scenario 4 Description

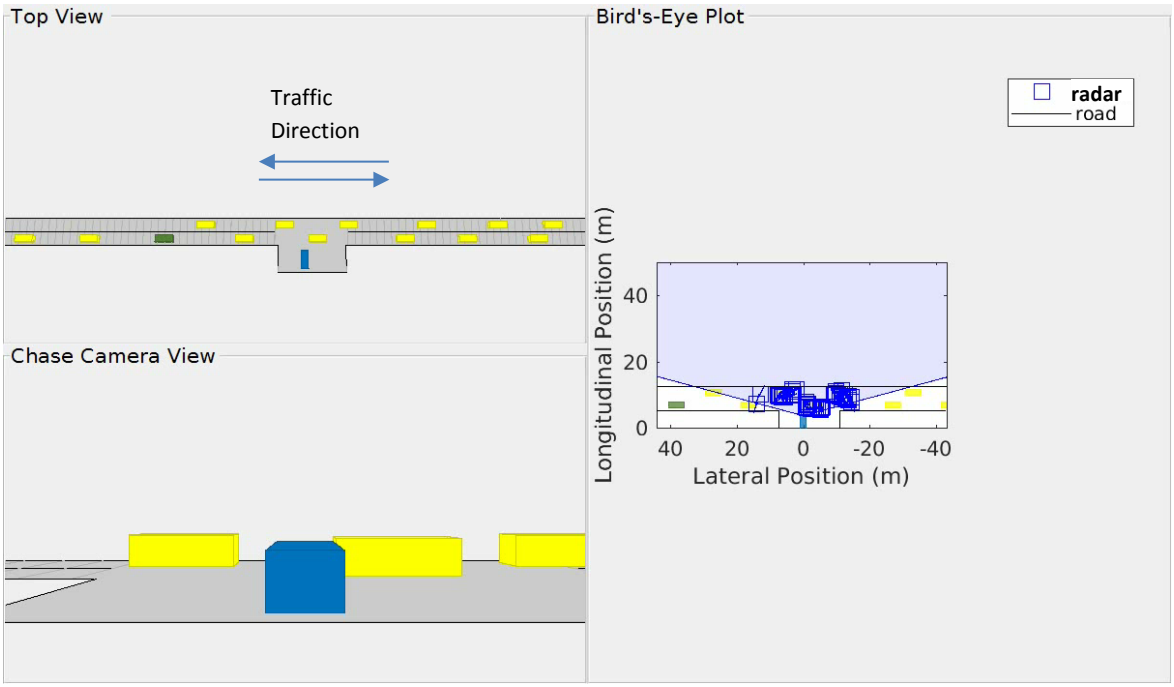

Figure 45: Position of vehicles at end of Scenario 4

The power levels for scenario 4 are tabulated in Table 11. The table shows that the power level of the interferer is higher than for the target in all cases. Looking at the plots in Figure 46, it is clear the difference between interferer and target is relative small, and that a wider band makes a significant difference in the amount of distance at which the target level rises above the interference level.

Table 11: Received power from reference target, clutter, and interference power in reference range bin, P_T, P_C, and P_I, respectively, for Scenario 4: Backing out of Parking Space

dB Watts	Ego Radar	Other Radar	P_T	P_C	P_I
76-77 GHz	SRR	LRR	-98	-121	-69
	SRR	MRR	-98	-121	-73
76-81 GHz	SRR	LRR	-98	-121	-76
	SRR	MRR	-98	-121	-80

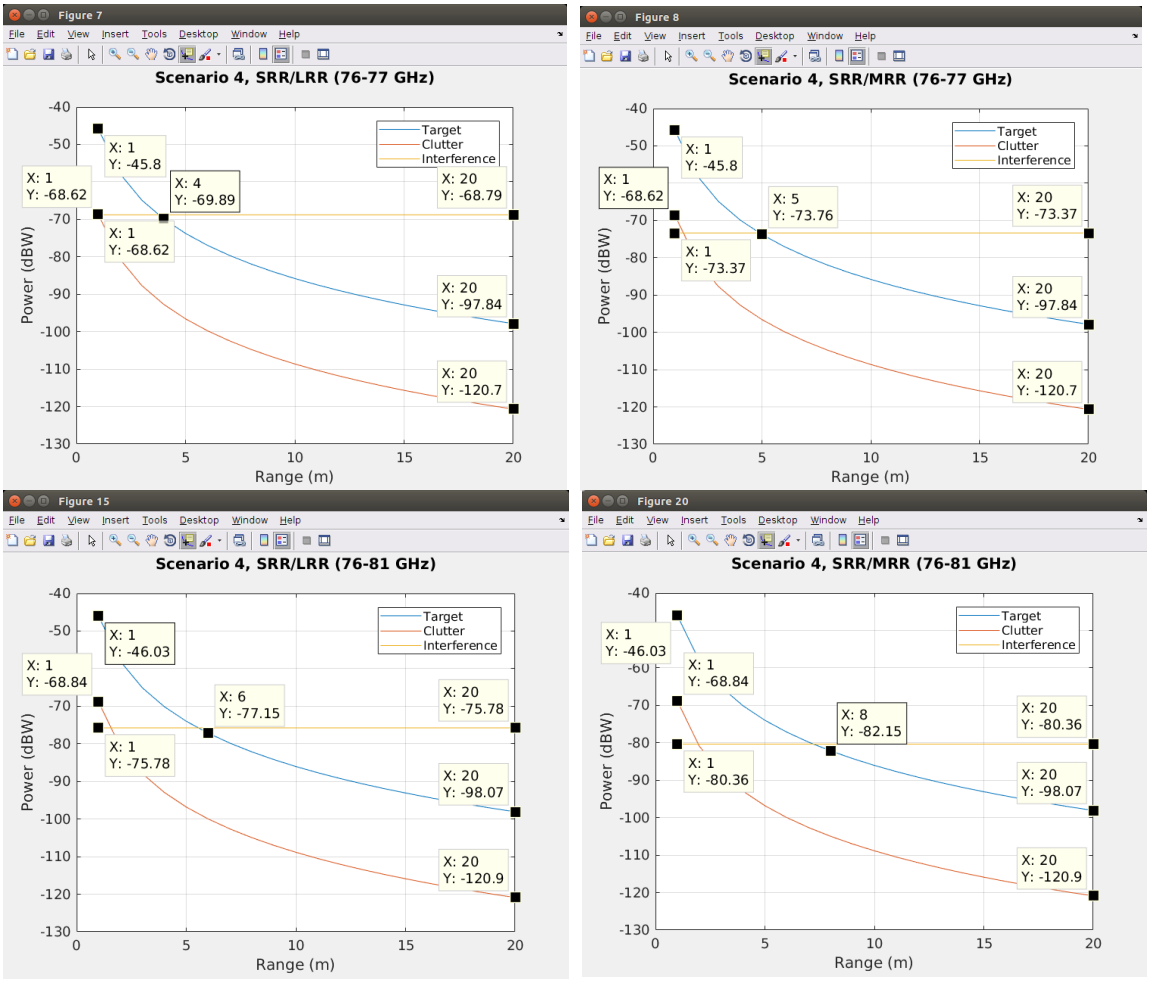

Figure 46: Comparison of target, clutter, and interferer power with various radars at various ranges

6.5.1 **Scenario 4 – Short versus long-range radar system impacts**

This version of scenario 4 examines the situation where the ego has a short-range radar and the interferer vehicles have long-range radars. It is obvious from the plots that, even in the no interferer case (Figure 47), the tracker is confusing detection from the non-target interferers with the target. The addition of the interference, Figure 48, shortens the detection distance, and causes an increase in the size of the error ellipses, which means that the Kalman filter in the tracker is having difficulty in making its predictions. Using the wider band, (Figure 49), does increase the distance at which detection first occurs.

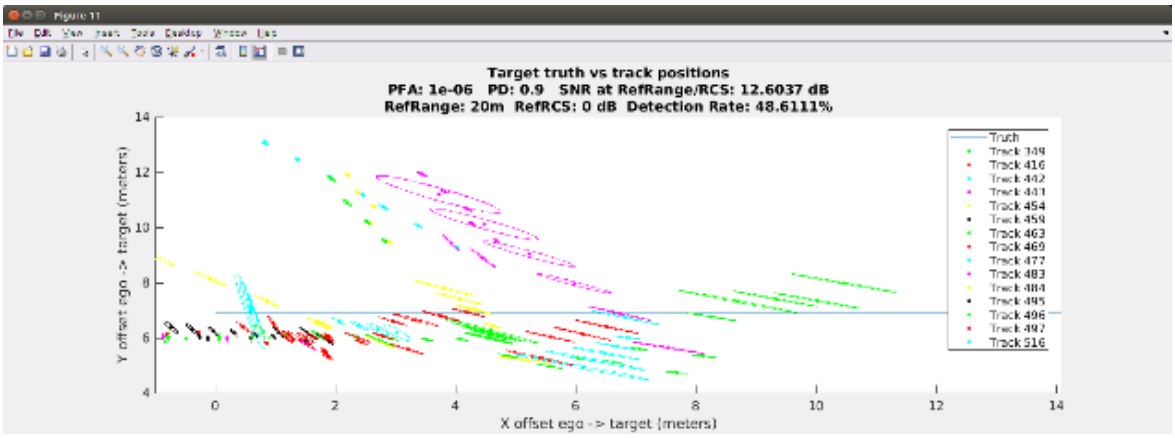

Figure 47: Plot of persistent target tracks from Scenario 4, short-range ego radar with no interference

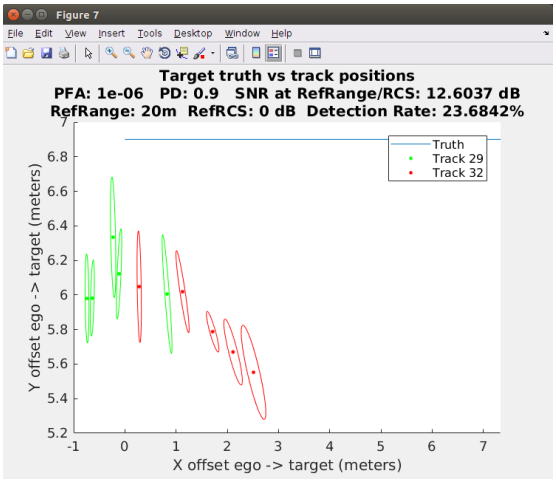

Figure 48: Plot of persistent target tracks from Scenario 4, short-range ego radar versus long-range interferer radar, with interference, for the case of 76-77 GHz band

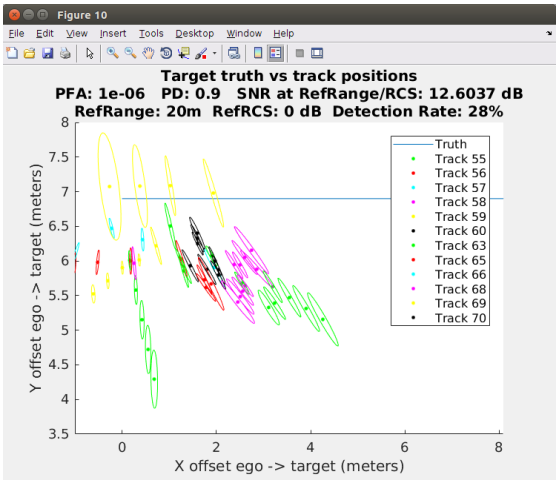

Figure 49: Plot of persistent target tracks from Scenario 4, short-range ego radar versus long-range interferer radar , with interference, for the case of 76-81 GHz band

6.5.2 **Scenario 4 – Short versus mid-range radar system impacts**

This version of scenario 4 examines the situation where the ego has a short-range radar and the interferer vehicles have mid-range radars. As with the long-range radar case, the tracker is confusing detection from the non-target interferers with the target (Figure 50). Similarly, the addition of the interference shortens the detection distance (Figure 51), however, using the wider band does not increase the distance at which detection first occurs (Figure 52).

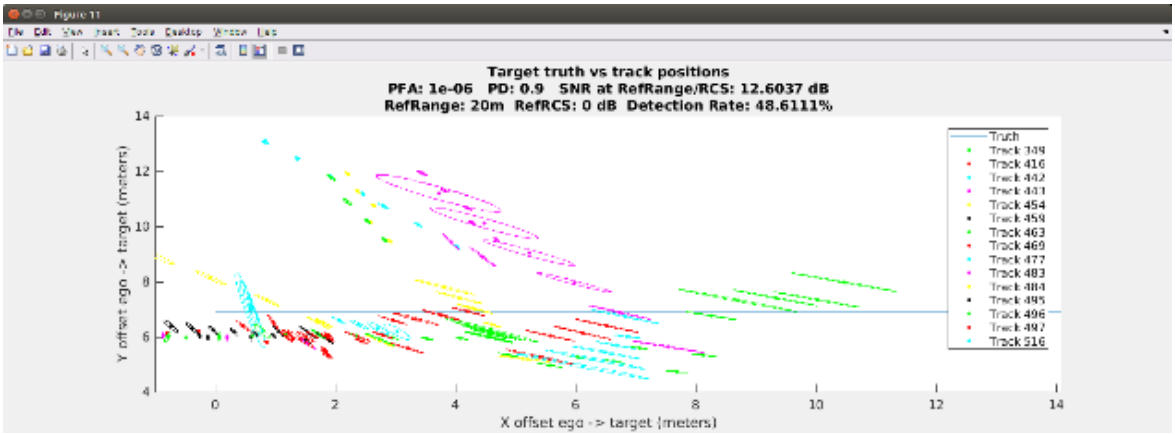

Figure 50: Plot of persistent target tracks from Scenario 4, short-range ego radar with no interference

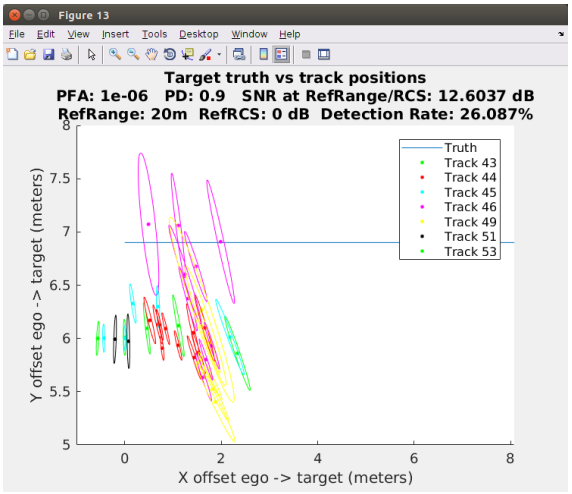

Figure 51: Plot of persistent target tracks from Scenario 4, short-range ego radar versus mid-range interferer radar, with interference, for the case of 76-77 GHz band

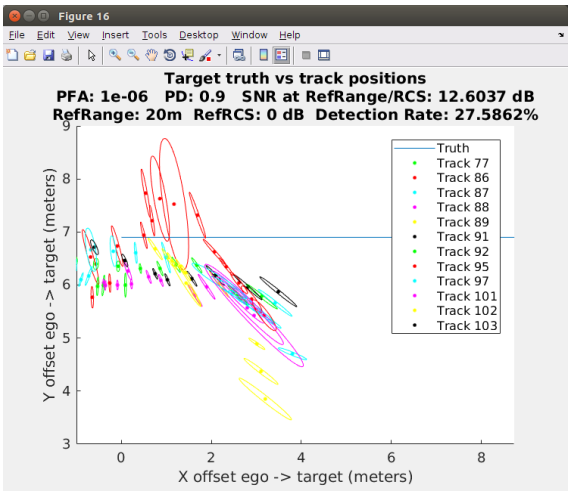

Figure 52: Plot of persistent target tracks from Scenario 4, short-range ego radar versus mid-range interferer radar, with interference, for the case of 76-81 GHz band

6.6 Scenario 5 – Rear-facing SRR and forward-facing LRR in traffic

Scenario 5 involves two radars.

- a rear-facing, short range radar
    - such as a blind-spot detector), and
- a forward-looking, long-range radar
    - such as a collision avoidance radar

Each radar faces the direct arrival from the other, as interference. Each needs to detect the reflection from the other, as target.

The power received at the ego vehicle, due to a reflection from the target $P_{RX,Ego}(R,\sigma)$ is given by the radar range equation as:

$$P_{RX,Ego}(R,\sigma) = \frac{P_{TX,Ego}G_{Ego}^2\lambda^2\sigma_{Int}}{(4\pi)^3R^4}$$

where

$P_{TX,Ego}$ is the power transmitted by the ego radar
G_{Ego} is the gain of the ego radar's antenna
λ is the wavelength of the RF carrier
σ_{Int} is the radar cross section of the other car
R is the range between the two radars

Whereas, the interference power $I_{RX,Ego}(R,\sigma)$ due to the radar on the other vehicle is given by Friis equation:

$$I_{RX,Ego}(R) = \frac{P_{TX,Int}G_{Ego}G_{Int}\lambda^2}{(4\pi)^2R^2}$$

where

$P_{TX,Int}$ is the power transmitted by the Interfering (other) radar
G_{Ego} is the gain of the ego radar's antenna
G_{Int} is the gain of the Interfering radar's antenna
λ is the wavelength of the RF carrier
R is the range between the two radars

First consider the forward-looking LRR facing the transmission of a rear-facing SRR, as depicted in Figure 53. The LRR is intended to see a 10 dBm^2 target at 175 meters, where the interference level is 25 dB above the target return power.

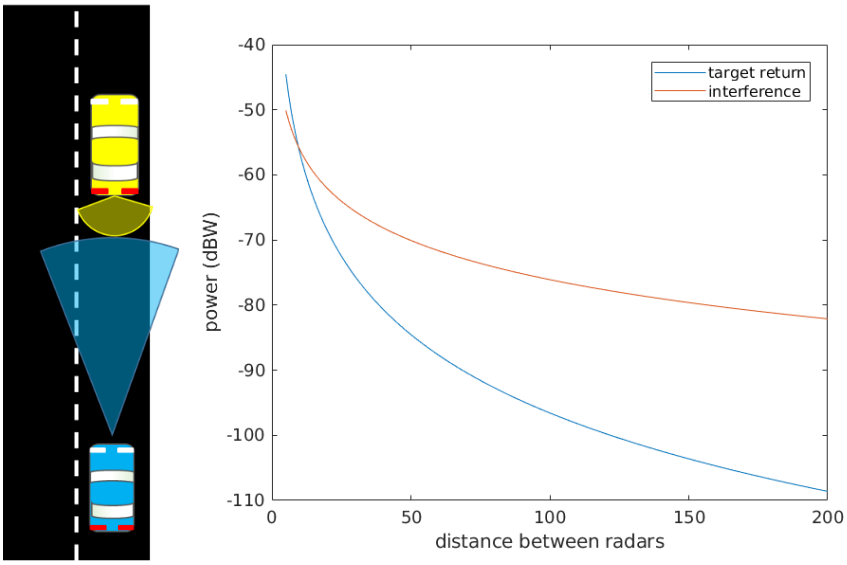

Figure 53: The forward-looking LRR on the ego vehicle (blue) faces direct illumination from a rear-facing SRR.

Next consider the rear-facing SRR facing the transmission of a forward-looking LRR, as depicted in Figure 54. The SRR is intended to see a 10 dBm^2 target at 35 meters, where the interference level is 52 dB above the target return power.

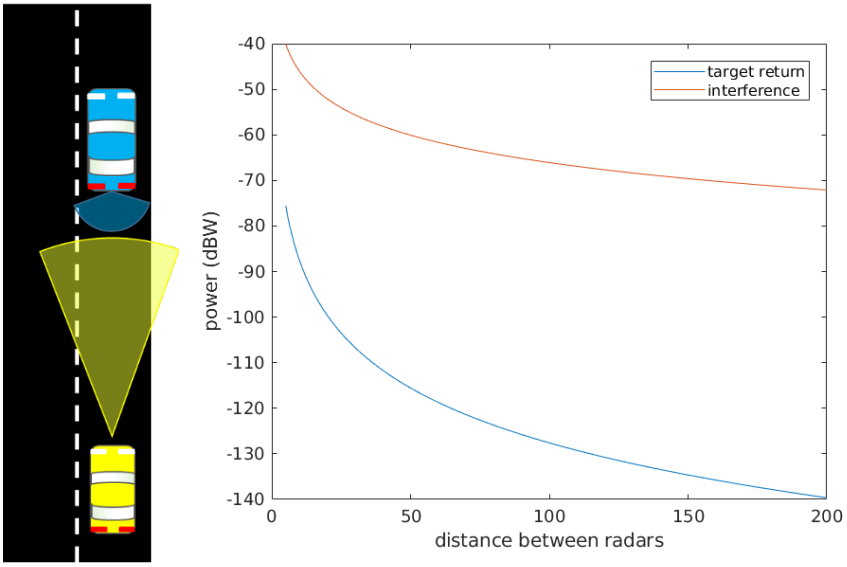

Figure 54: The rear-facing SRR on the ego vehicle (blue) faces direct illumination from a forward-looking LRR.

If both the LRR and SRR choose their carrier frequency at random over the available band, and are not synchronized, then the statistical overlap Is the same as for the larger of the pair

In the case of 76-77 GHz, the expected signal to interference plus noise ratio (SINR) for the LRR is -21 dB, and for the SRR it is -48 dB.

In the case of 76-81 GHz, the expected SINR for the LRR is -17 dB, and for the SRR it is, -44 dB.

The case of the SRR subject to direct illumination by the LRR presents extremely challenging levels of interference to mitigate and suggests that measures should be taken to ensure that rear-facing and forward-looking radar cooperate to not interfere. One recommendation is to divide the available frequency band for rear and forward directions.

6.7 Results

The results above are detailed above are reduced to a pair of tables, where the SINR is computed at the reference range of the ego radar. Table 12 tabulates the SINR and reduction in terminal track values for radars sharing the 76-77 GHz band. Table 13 tabulates the SINR and reduction in terminal track values for radars sharing the 76-81 GHz band. A terminal track is a series of updated measurements which is maintained all the way to the time of collision. The column, Track Range, contains the range at which a terminal track is formed in the simulation with interference as a percentage of the range at which the terminal track was formed in the simulation without interference.

For our simulations, interference is modeled as Gaussian noise distributed across the receiver's range bins. This means that the interfering radars are assumed to use waveforms that do not correlate. This means that no false alarms are generated by cross-correlating the waveforms.

The three radars are modeled using the parameters in Table 5. The simulations use the base track assumptions in MATLAB's ADAS toolbox.

Table 12: SINR and impact on track range for the scenarios using the 76-77 GHz band.

Scenario	Band	Victim Radar	Interfering Radar	SINR	Track Range
1	76-77	LRR	LRR	-38	11%
1	76-77	MRR	MRR	-35	33%
2	76-77	LRR	LRR	3	100%
2	76-77	MRR	MRR	0	88%
3	76-77	LRR	LRR	-11	100%
3	76-77	MRR	MRR	-5	65%
4	76-77	SRR	LRR	-30	25%
4	76-77	SRR	MRR	-25	23%
5	76-77	LRR	SRR	-21	
5	76-77	SRR	LRR	-48	

Table 13: SINR and impact on track range for the scenarios using the 76-81 GHz band.

Scenario	Band	Victim Radar	Interfering Radar	SINR	Track Range
1	76-81	LRR	LRR	-31	16%
1	76-81	MRR	MRR	-28	44%
2	76-81	LRR	LRR	10	100%
2	76-81	MRR	MRR	23	94%
3	76-81	LRR	LRR	-4	100%
3	76-81	MRR	MRR	2	70%
4	76-81	SRR	LRR	-22	41%
4	76-81	SRR	MRR	-18	34%
5	76-81	LRR	SRR	-17	
5	76-81	SRR	LRR	-44	

7 Recommendations for Test Development

7.1 Tests for model validation

The models in this research effort estimate mean interference power as expected from free space propagation using generic radar models. These are useful in estimating expected levels, and identifying situations that present high levels of interference. However, the real operating environment for automotive radar is clutter filled, dynamic, and a variety of systems may be operating in close proximity. For this reason, a set of tests, which measure the interference energy in real situations akin to the scenarios computed here would allow these models to be evaluated, and ultimately, corrected for real world conditions.

7.1.1 **Interference from opposing traffic**

The model derived for interference from forward-looking radars in opposing traffic is derived in (Al-Hourani ,2017):

$$I_1 = \xi\lambda \int_{\delta}^{\infty} \frac{P_0\gamma_1}{L^2 + r^2}\, dr = \frac{\xi\lambda P_0\gamma_1}{L}\left(\frac{\pi}{2} - \arctan(\delta/L)\right),$$

The interference power present in the real world can be measured on a test track as shown in Figure 55. The ego vehicle, in blue, is replaced by a passive radiometer that measures power in the 76-81 GHz band. The test can be repeated to develop empirical distributions for the fluctuation model, and run at different locations to understand variation due to environment.

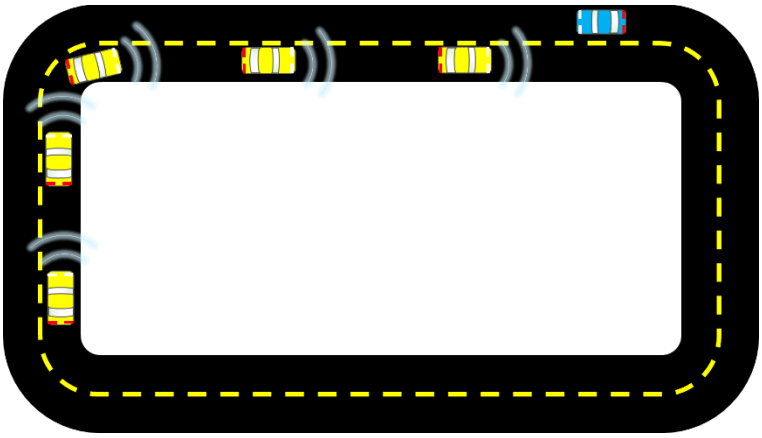

Figure 55: A test track with five vehicles used to measure interference power similar to that estimated in Scenario 1.

7.1.2 **Interference from passing traffic**

The model derived for interference from forward-looking radars passing the ego vehicle is derived as:

$$I_2 = \xi\lambda \int_{\delta}^{\infty} \frac{P_0\gamma_1\gamma_2}{R^2(L^2+r^2)}dr = \frac{\xi\lambda P_0\gamma_1\gamma_2}{R^2 L}\left(\frac{\pi}{2} - \arctan(\delta/L)\right),$$

The interfering vehicles, in yellow, illuminate a green vehicle in the shared field of view, as the ego vehicle, in blue. This is shown in Figure 56. The test can be repeated to develop empirical distributions for the fluctuation model, and run at different locations to understand variation due to environment.

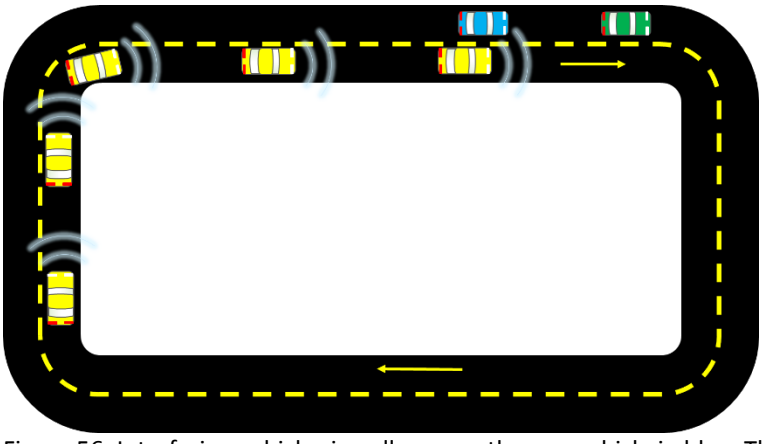

Figure 56: Interfering vehicles in yellow pass the ego vehicle in blue. The radiometer on the blue vehicle measures energy from the radars, including that which is reflected from the green target car.

7.2 Tests for evaluation of fielded systems

The development of automotive safety test for fielded systems should consider their robustness to congested environments. A major concern is the possible combinations of systems presents an

infeasible number of tests to conduct. Reasonable subsets of these combinations could be chosen, based on market penetration of particular models, or the tests could be conducted with two subsets,

1. transmitters that use identical waveforms, and
2. transmitters that emit white noise.

The simulated scenarios here are intended to identify situations with significant interference levels, which, without mitigation, present a problem for normal radar operation. The situations identified as having significant interference in Table 12 and Table 13 are the Scenarios labelled 1, 4, and 5.

- Scenario 1: Opposing traffic for LRR and MRR
- Scenario 4: Backing out from parking space supported by SRR
- Scenario 5: Blind-spot detection radar, SRR, in traffic ahead of forward-looking LRR

The configurations in these scenarios should be adapted for automotive safety tests, which evaluate system functions that may rely on radar: forward collision warning, blind-spot detection, and rear-view parking assistance.

8 Discussion

8.1 Review

The radar congestion study

- identified trends in automotive radars, through interviews with industry and review of scholarly literature,
- developed models for expected interference levels,
- adapted MATLAB ADAS to simulate scenarios with interference, and
- developed initial experimental designs for experiments to
    - amend theoretical models, and
    - evaluate mitigation strategy effectiveness in deployed systems.

8.2 Study conclusions

The radar congestion study characterizes the environment in which automotive radars must operate, as systems with greater autonomy enter the market. Systems that operate well in environments with few other radars may suffer significant degradation of performance in radar congested environments. The results of the study show, levels of interference based on operation of current systems in congested environments will be significant. In scenarios with many vehicles operating radars in the 76-81 GHz band, the power from other radars will likely exceed the power of echoes from targets needed for specified performance, by several orders of magnitude.

The modeling and simulation work focused on two questions.

- How much power does, a given radar, receive from other radar transmitters?
- How does this impact the performance of a collision warning system?

The first question is addressed by developing a model for nominal automotive radars and computing the amount of power overlapping in space, time, and spectrum. This work is done theoretically, assuming free space propagation of RF waves.

The study identified multiple scenario, which require radar system designs to mitigate significant levels of mutual interference. Of the five scenarios studied, three presented significant levels of interference, and these should be studied empirically:

- forward-looking radars operating in presence of opposing traffic
- short-range radars for backing out of parking spaces confronting radars in traffic
- rear-looking (such as blind-spot detection) radars in traffic with forward-looking radars

The fidelity of the free space propagation models used in this study could be improved with the development of empirical channel models for automotive applications at 76-81 GHz. Measurements of representative environments can provide a better understanding of the physical channel, and variation of waveforms transmitted in 76-81 GHz.

The second question has been addressed by introducing the power computed for the interference, as noise, into a system simulation. This approach is common in past studies, and assumes the waveforms of the interfering radar are substantially different, so that their mutual energy does not correlate. This approach is taken, in part, because it requires a minimum of assumptions about the signal processing chain behind the receiving radar's front end. To quantify possible system impacts, the processing functions were based on a generic model developed in cooperation with industry professionals and simulated in MATLAB's ADAS Toolbox. The simulations show that for some combinations of radar ranges in certain scenarios, the performance can be significantly impacted in terms of the effect on the metrics selected for this study:

- Increase in SINR, and
- Decrease in terminal track range.

In general, an increase in SINR, increases the number of errors to be expected by the detector. While many of the errors in the detector may be mitigated with further signal processing, the chances of system errors, statistically, increases. The reduction in formation of the terminal track is proposed for this study because it shows that the system's performance is degraded, from the perspective that it no longer responds as quickly and reliably. However, again, this is a statistical statement, and not easily tied to the particulars of a given integrated control system.

The study here ignored the possible impact of radars transmitting similar waveforms, and restricted the impact of mutual interference as a source of added noise. This follows prior work, including (John & Schipper, 2012; Heuel, 2016; Al-Hourani, Evans, Kandeepan, Moran, & Eltom, 2017). The impact of specific waveforms and system architectures could be addressed through empirical testing. The scenarios developed in this study could be adapted as the basis for empirical tests of interference prone situations involving radars of similar waveform. The suggested scenarios would correspond to automotive functions that rely on radar, including forward collision warning, blind spot detection, and rear-view parking assist.

9 Bibliography

Al-Hourani, A., Evans, R. J., Kandeepan, S., Moran, B., & Eltom, H. (2017). Stochastic geometry methods for modeling automotive radar interference. *IEEE Transactions on Intelligent Transportation Systems*. 2017.

Buller, W. T., & LeBlanc, D. J. (2012). Radar characterization of automobiles and surrogate test-targets for evaluating automotive pre-collision systems. In *Proceedings of the 2012 IEEE International Symposium on Antennas and Propagation*, July 8-14, 2012, Chicago, pp. 1-2.

Grace, N. (2017, July 13). FCC unlocks new airwaves for vehicular radar use (Press release). Washington, DC: Federal Communications Commission. Available at https://apps.fcc.gov/edocs_public/attachmatch/DOC-345778A1.pdf

Haenggi, M., & Ganti, R. K. (2008). Interference in large wireless networks. *Foundations and Trends in Networking*, *3*(2), pp.127-248.

Heuel, S. (2016). Automotive radar sensors must address interference issues. *Microwave Journal; 59*(12), pp. 22-36.

John, A., & Schipper, T. (2012, December 21). *MOre Safety for All by Radar Interference Mitigation D5.4 – Conclusion and outlook how to solve still open challenges* (Part 4 of 4 parts. Report No. MOSARIM No. 248231). Brussels, Belgium: European Commission. Available at https://cordis.europa.eu/docs/projects/cnect/1/248231/080/deliverables/001-Deliverable54final.pdf

Kissinger, D. (2012). *Millimeter-wave receiver concepts for 77 GHz automotive radar in silicon-germanium technology*. New York: Springer Science & Business Media, LLC.

Kunert, M. (2012, December 21). More Safety for All by Radar Interference Mitigation Project Final Report – Publishable Summary. Brussels, Belgium: European Commission. Available at https://cordis.europa.eu/docs/projects/cnect/1/248231/080/deliverables/001-D611finalreportfinal.pdf

Levanon, N., & Mozeson, E. (2004). *Radar signals.* Hoboken, NJ: Wiley-Interscience.

National Highway Traffic Safety Administration & Insurance Institute for Highway Safety. (2016, March 17). *U.S. DOT and IIHS announce historic commitment of 20 automakers to make automatic emergency braking standard on new vehicles* [Joint press release]. Retrieved from www.iihs.org/iihs/news/desktopnews/u-s-dot-and-iihs-announce-historic-commitment-of-20-automakers-to-make-automatic-emergency-braking-standard-on-new-vehicles

Richards, M. A. (2005). *Fundamentals of radar signal processing*. New York: McGraw-Hill Education.

Sarabandi, K., Li, E. S., & Nashashibi, A. (1997). Modeling and measurements of scattering from road surfaces at millimeter-wave frequencies. *IEEE Transactions on Antennas and Propagation 45.11*: 1679-1688.

Sturm, C., Sit, Y. L., Braun, M., & Zwick, T. (2013). Spectrally interleaved multi-carrier signals for radar network applications and multi-input multi-output radar. *IET Radar, Sonar & Navigation 7.3*): 261-269.

Tyson, T. (2013) Detection of Signals in Noise. (Physics lecture notes, University of California at Davis). Retrieved from https://*123.physics.ucdavis.edu/week_5_files/filters/matched_filter.pdf*

Appendix A: Evaluation of Mitigation Strategies From MOSARIM

Estimation of interference suppression impact, produced by the MOSARIM study in 2012, is shown in Table 14. Cells in **ORANGE** were not tested, so margin is only an estimate.

Table 14: Ranking list of mitigation techniques from MOSARIM study (Kunert, 2012)

ID	Counter Measure	Interference Reduction	Comment
T3.1	CFAR (constant false alarm rate) for interference mitigation	ca. 10 -20 dB	It can be used for all kind of functions without any constraints. CFAR performance slightly influence by number of targets
T6.5	Detect interference and change transmit frequency range of chirps	Up to infinity dB	Infinite mitigation margin can be obtained for 2 radars, but will be reduced if many interferers are present and band overlapping occurs. Efficiency depends on the occupied bandwidth and the bandwidth available
T2.1	Using pauses of random length between chirps or pulses	only a few dB	Suppression of ghost targets and results in increase of noise floor. Typically measurement to pause ratio is maximum 50% => on average 3 dB mitigation margin
T3.4	Application of driving direction specific pre-defined frequency band separation	up to infinity dB for same driving direction, but no mitigation margin for crossing traffic	This needs worldwide coordination to become effective. For crossing traffic a special measure has to be found.
T6.2	Detect interference and repair Rx results (Time domain)	up to ca. 20 dB possible	The influence of fast or slow crossing FM chirps still needs further investigation on mitigation margin impact
T2.2	Using random sequence of chirp types (Up-chirp, Down-chirp, CW-Chirp)	Only a few dB	Suppression of ghost targets and results in increase of noise floor. Only limited mitigation margin capability if done in the same frequency range
T5.4	Digital Beam Forming	Only a few dB	Mitigation effect depends on beamwidth (space domain)
T6.4	Detect interference and change timing of transmit chirp or pulses	a large number of dB is expected	With good timing and arrangement of FM ramps high margin can be reached. A prerequisite is that all radars use same ramp duration to make synchronization without ramp crossing possible
T1.2	Specific polarisation following the Radar location (frontal, rear, side)	typically ca. 15 dB for co-to cross-polarization (linear)	This is already partially used for ACC radars that have 45 degree slant polarization (reduced interference from oncoming radars by 15 dB)

Appendix B: Matlab ADAS Toolbox, Radar, and Tracker Objects

1. Long-range radar:

radarDetectionGeneratorSNR with properties:

SensorIndex: 1
UpdateInterval: 0.0500

SensorLocation: [3.7000 0]
Height: 0.2000
Yaw: 0
Pitch: 0
Roll: 0

FieldOfView: [20 5]
MaxRange: 250
RangeRateLimits: [-100 100]

DetectionProbability: 0.9000
FalseAlarmRate: 1.0000e-06
ReferenceRange: 100
ReferenceRCS: 0

AzimuthResolution: 5
RangeResolution: 0.7495
RangeRateResolution: 0.5000

AzimuthBiasFraction: 0.1000
RangeBiasFraction: 0.0500
RangeRateBiasFraction: 0.0500

HasElevation: false
HasRangeRate: true
HasNoise: true
HasFalseAlarms: true
MaxNumDetectionsSource: 'Auto'
DetectionCoordinates: 'Ego Cartesian'

ActorProfiles: [33Ã—1 struct]

2. Medium-range radar:

radarDetectionGeneratorSNR with properties:

SensorIndex: 1
UpdateInterval: 0.0500

SensorLocation: [3.7000 0]
Height: 0.2000
Yaw: 0
Pitch: 0
Roll: 0

FieldOfView: [90 10]
MaxRange: 100
RangeRateLimits: [-100 100]

DetectionProbability: 0.9000
FalseAlarmRate: 1.0000e-06
ReferenceRange: 50
ReferenceRCS: 0

AzimuthResolution: 15
RangeResolution: 0.3747
RangeRateResolution: 0.5000

AzimuthBiasFraction: 0.1000
RangeBiasFraction: 0.0500
RangeRateBiasFraction: 0.0500

HasElevation: false
HasRangeRate: true
HasNoise: true
HasFalseAlarms: true
MaxNumDetectionsSource: 'Auto'
DetectionCoordinates: 'Ego Cartesian'

ActorProfiles: [33Ã—1 struct]

3. Short-range radar:

radarDetectionGeneratorSNR with properties:

SensorIndex: 1
UpdateInterval: 0.0500

SensorLocation: [3.7000 0]
Height: 0.2000
Yaw: 0
Pitch: 0
Roll: 0

FieldOfView: [150 10]
MaxRange: 80
RangeRateLimits: [-100 100]

DetectionProbability: 0.9000
FalseAlarmRate: 1.0000e-06
ReferenceRange: 20
ReferenceRCS: 0

AzimuthResolution: 50
RangeResolution: 0.2998
RangeRateResolution: 0.5000

AzimuthBiasFraction: 0.1000
RangeBiasFraction: 0.0500
RangeRateBiasFraction: 0.0500

HasElevation: false
HasRangeRate: true
HasNoise: true
HasFalseAlarms: true
MaxNumDetectionsSource: 'Auto'
DetectionCoordinates: 'Ego Cartesian'

ActorProfiles: [18Ã—1 struct]

4. Tracker

multiObjectTracker with properties:

FilterInitializationFcn: 'initcvkf'
AssignmentThreshold: 30
ConfirmationParameters: [2 3]
NumCoastingUpdates: 5
MaxNumTracks: 200
HasCostMatrixInput: false
NumTracks: 0
NumConfirmedTracks: 0

DOT HS 812 632
September 2018

U.S. Department
of Transportation

**National Highway
Traffic Safety
Administration**

13790-092518-v2b